Science of the Total Environment 929 (2024) 172602

Contents lists available at ScienceDirect

Science of the Total Environment

journal homepage: www.elsevier.com/locate/scitotenv

Review

Arsenic and antimony desorption in water treatment processes: Scaling up challenges with emerging adsorbents

Mariko A. Carneiro *, Ariana M.A. Pintor, Rui A.R. Boaventura, Cidália M.S. Botelho

Laboratory of Separation and Reaction Engineering, Laboratory of Catalysis and Materials (LSRE-LCM), Department of Chemical Engineering, Faculty of Engineering, University of Porto, Rua Dr. Roberto Frias, 4200-465 Porto, Portugal
ALiCE - Associate Laboratory in Chemical Engineering, Faculty of Engineering, University of Porto, Rua Dr. Roberto Frias, 4200-465 Porto, Portugal

HIGHLIGHTS

- The chemical desorption of As and Sb from spent adsorbents was reviewed.
- The most common eluents for As and Sb are NaOH and HCl, respectively.
- Desorption efficiencies of many types of adsorbents were summarized.
- Regeneration cycles in batch and continuous mode were discussed.
- Knowledge gaps, current challenges, and future research needs were identified.

GRAPHICAL ABSTRACT

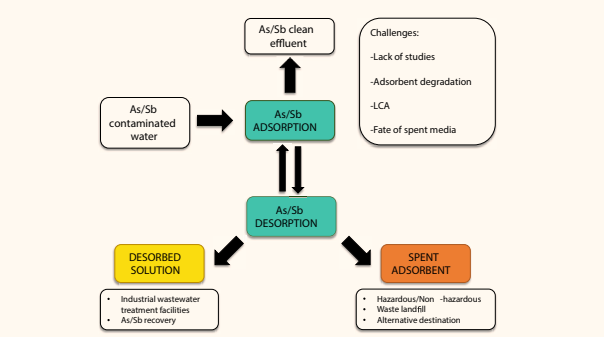

ARTICLE INFO

Editor: Bo Gao

Keywords:
Metalloids
Adsorption
Regeneration
Water treatment
Eluents

ABSTRACT

The metalloids arsenic (As) and antimony (Sb) belong to the pnictogen group of the periodic table; they share many characteristics, including their toxic and carcinogenic properties; and rank as high-priority pollutants in the United States and the European Union. Adsorption is one of the most effective techniques for removing both elements and desorption, for further reuse, is a part of the process to make adsorption more sustainable and feasible. This review presents the current state of knowledge on arsenic and antimony desorption from exhausted adsorbents previously used in water treatment, that has been reported in the literature. The application of different types of eluents to desorb As and Sb and their desorption performance are described. The regeneration of saturated adsorbents and adsorbate recovery techniques are outlined, including the fate of spent media and possible alternatives for waste disposal of exhausted materials. Future research directions are discussed, as well as current issues including the lack of environmental impact analysis of emerging adsorbents.

1. Introduction

Arsenic (As) and antimony (Sb) are both metalloids from the

* Corresponding author at: Laboratory of Separation and Reaction Engineering – Laboratory of Catalysis and Materials (LSRE-LCM), Department of Chemical Engineering, Faculty of Engineering, University of Porto, Rua Dr. Roberto Frias, 4200-465 Porto, Portugal.
E-mail address: mariko.carneiro@fe.up.pt (M.A. Carneiro).

https://doi.org/10.1016/j.scitotenv.2024.172602
Received 15 February 2024; Received in revised form 9 April 2024; Accepted 17 April 2024
Available online 21 April 2024

Abbreviations

List of acronyms

DE	Desorption
EDTA	Ethylenediaminetetraacetic acid
HRT	Hydraulic Retention Time
LCA	Life Cycle Assessment
MOFs	Metal-Organic Frameworks
MTZ	Mass Transfer Zone
PET	Polyethylene Terephthalate
PFAS	Poly- and Perfluoroalkyl Substances
STLC	Soluble Threshold Limit Concentration
TCLP	Toxicity Characteristic Leaching Procedure
TTLP	Total Threshold Limit Concentration
USPHS	US Public Health Service
WHO	World Health Organization
WTRs	Water Treatment Residues

List of symbols

a	initial rate of adsorption/desorption (mg g^{-1} h^{-1})
b	coverage scale factor that corresponds to the reciprocal of the coverage at which the adsorption/desorption rate has fallen to 1/e of its initial value (g mg^{-1})
C	concentration of adsorbate left in the solution (mg L^{-1})
k_2	pseudo-second-order kinetic constant (g mg^{-1} h^{-1})
m	mass of adsorbent (g)
q_a	adsorption capacity (mg g^{-1})
q_d	desorption capacity (mg g^{-1})
d_e	desorption efficiency (%)
q_{loss}	reduction in the adsorption capacity (%)
q_o	initial adsorption capacity of the fresh adsorbent (mg g^{-1})
q_r	adsorption capacity after regeneration (mg g^{-1})
r^2	coefficient of determination
V	solution volume (L)

pnictogen group of the periodic table. They share a lot of characteristics including being very toxic for humans, carcinogenic and classified as high-priority pollutants by the European Union and the United States (Guo et al., 2014). They can exist naturally in the environment, and are often combined; nevertheless, anthropogenic activities are also responsible for their occurrence in waters at hazardous levels. The World Health Organization (WHO) recommends limit concentrations in drinking water as 10 μg L^{-1} and 20 μg L^{-1} for As and Sb, respectively (WHO, 2022). However, stricter regulations may be found in the United States, the European Union, and China ((MOH), M.o.H.o.t.P.s.R.o.C, 2006; EPA, 2002; European Union, C, 2020).

The most predominant forms of arsenic and antimony in the environment are the inorganic species (iAs, iSb) found in two main oxidation states: trivalent (As(III), Sb(III)) and pentavalent (As(V), Sb(V)), which are most commonly combined with sulfur, oxygen and/or iron (Pintor et al., 2018; Qi and Pichler, 2017). The more oxidized species are usually found under oxic conditions, just as the more reduced species are found under anoxic conditions (Müller et al., 2022; Smichowski et al., 1998; Gebel, 1997). The trivalent forms of both species are considered more toxic to humans (Pintor et al., 2020) and are usually harder to remove from water.

Since As and Sb are toxic, pose a threat to human health, and are subject to legal limits, the removal of As and Sb from water and wastewater is mandatory (Pintor et al., 2022). Coagulation/flocculation, ion exchange, membrane separation, chemical oxidation, electrochemical methods, phytoremediation, bioremediation, biofiltration, and adsorption are some of the technologies used to remove As and Sb from water (Ungureanu et al., 2015). Adsorption is considered one of the most attractive water treatment technologies due to its simple design requirements, high removal efficiency, low cost, and easy operation (Alka et al., 2021; Long et al., 2020a). Activated carbon, activated alumina, and ion exchange resins are the most common and commercially available adsorbents (Ungureanu et al., 2015). The use of non-conventional adsorbents, such as natural biomass-based materials and novel functional composites, can increase the cost-effectiveness and the environmental friendliness of the adsorption process.

Mathematical models based on the nature of adsorbate-adsorbent interactions and bed profiles have been developed to predict the operation of an adsorption system (Xu et al., 2013). After a certain operation time (which varies depending on the operational conditions, sorbent type, and effluent characteristics) the adsorbent becomes saturated and must be replaced or treated via a regeneration process before it can be reused (Alka et al., 2021). Many benefits are associated with the regeneration of saturated adsorbents, including economic savings and reduced environmental impact (Vakili et al., 2019). In terms of environmental and economic feasibility, the adsorption process is dependent on the reuse of the exhausted adsorbent through regeneration and, in certain circumstances, the recovery of a valuable adsorbate, such as antimony, from the saturated bed. When the adsorbent or adsorbate is easily obtainable at low cost, desorption may not be economically viable; nevertheless, desorption can be a more ecologically friendly alternative.

Adsorbent regeneration may be achieved by thermal, chemical, biological, and ozonation processes. Chemical or solvent desorption (DE) is generally viewed as the most cost-effective method (Patel, 2021). Like adsorption, desorption can be conducted in batch or continuous (column) mode, and the solvent solution is also known as the eluent. Acids, bases, salts, and complexing agents are different categories of chemicals accessible for use as eluents. A successful desorption process is dependent on the appropriate selection of eluent type and concentration, which is primarily determined by the adsorbent material and the respective adsorption mechanism to the adsorbent (Lata et al., 2015).

Several review papers have explored the adsorption of arsenic by various types of adsorbents, including iron and aluminum-based adsorbents (Giles et al., 2011; Gallegos-Garcia et al., 2012), titanium dioxide (Yan et al., 2016; Guan et al., 2012), rare-earth-based materials (Yu et al., 2018), graphene-based materials (Yang et al., 2016), activated carbons (Meez et al., 2021; Deliyanni et al., 2015; Mondal and Garg, 2017), biochars (Srivastav et al., n.d.), modified natural materials (Asere et al., 2019; Yeo et al., 2021), nano adsorbents (Patel et al., 2019; Siddiqui et al., 2019; Habuda-Stanic and Nujic, 2015; Lata and Samadder, 2016), functional sorbents (Liu et al., 2020), lignocellulosic materials (Maia et al., 2021), chitosan-derivatives (Pontoni and Fabbricino, 2012), biopolymer-based hydrogels (Pathan and Bose, 2020), and hydrotalcite (Dias and Fontes, 2020). However, few reviews have explored the adsorption of antimony. Some researchers have focused on adsorbent categories such as iron-based adsorbents (Deng et al., 2017; Yang et al., 2017) and carbon-based nanomaterials (Hu et al., 2021); while others have generally studied various types of adsorbents (Ungureanu et al., 2015; Cheng et al., n.d.).

The desorption and recovery of heavy metals (Vakili et al., 2019; Lata et al., 2015), as well as the desorption of organic pollutants (Baskar et al., 2022), and more specifically poly- and perfluoroalkyl substances (PFAS) (Gagliano et al., 2020), have been covered in reviews. Although arsenic desorption has been briefly reported (Lata et al., 2015; Carneiro et al., 2022a), the status of pnictogen desorption and recovery, such as arsenic and antimony, has not yet been investigated.

To fill this gap, this paper discusses the current state of the art of chemical desorption of arsenic and antimony oxyanions from exhausted media, including the eluent effect, regeneration and recovery,

challenges, and future perspectives. The paper is organized in sections presenting a short bibliometrics on the topic (Section 2), followed by a brief description of the adsorption of pnictogens (Section 3). The desorption parameters in batch and continuous mode are presented in Section 4, and the desorption mechanism is discussed in Section 5. Section 6 presents the last studies on arsenic desorption reported in the literature, followed by Section 7 which presents the same for antimony desorption. Batch vs continuous mode desorption is discussed in Section 8. Sections 9 and 10 discuss the regeneration and fate of spent adsorbent, as well as the recovery and fate of desorbed solution, respectively. Lastly, Section 11 outlines the current challenges on the topic and Section 12 draws conclusions according to the findings.

2. Short bibliometrics

A brief bibliometric study on As and Sb adsorption and desorption was carried out in the Web of Science and Scopus databases, in January 2024. The terms "arsenic AND adsorption AND water", "arsenic AND desorption AND water", "antimony AND adsorption AND water", and "antimony AND desorption AND water" were selected. The findings are represented in Fig. 1.

The number of publications on "arsenic AND adsorption AND water" is almost ten times higher than that on "antimony AND adsorption AND water". This might be supported by the fact that arsenic contamination in drinking water is a much older concern than antimony contamination. Arsenic's first regulation in water was established by the U.S. Public Health Service (USPHS) in 1942, with a recommended value of 50 μg L^{-1} (Pontius, 1994; USPHS, 1943), which was later reduced to 10 μg L^{-1} in 1962 (Smith and Smith, 2004). Furthermore, it was included in the first international standard for drinking water, published by the World Health Organization in 1958 with a maximum allowable concentration of 0.2 mg L^{-1} (World Health, O, 1958). Antimony, on the other hand, received its first WHO recommendation over 50 years later, in 1993, of 5 μL^{-1} for drinking water (World Health, O, 1993), which was modified to 20 μg L^{-1} in the 2017 edition (WHO, 2017).

Another reason for the higher number of academic papers addressing arsenic adsorption, than those focusing on antimony adsorption, is the larger population impacted by arsenic pollution in drinking water. It is estimated that arsenic-contaminated waters affect >230 million people globally, with a substantial part of the population being from developing nations (Shaji et al., 2021). Adsorption as a technology for arsenic removal from water is attractive for these nations since it is considered both inexpensive and effective (Dudek and Kołodyńska, 2022; Patel, 2019).

Antimony pollution is also a worldwide issue, although the population exposed to antimony-contaminated water has not yet been estimated. Contamination of water resources in the vicinity of shooting-range soils and mining sites with Sb is a problem in countries such as China, the U.S., and Spain, among other economic powers (Li et al., 2018; Bolan et al., 2022), which should be encouraged to develop and implement more robust and expensive water treatment solutions.

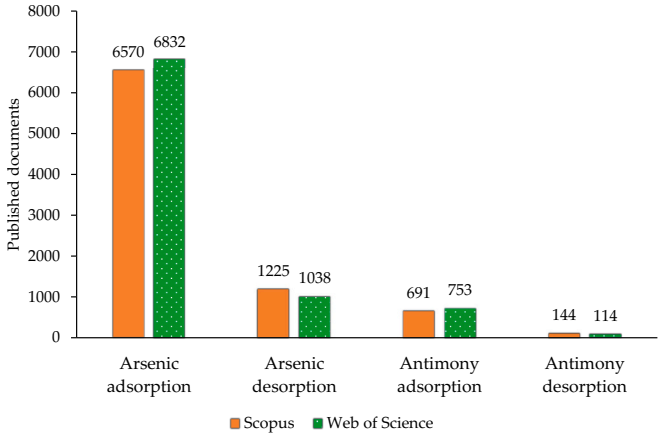

Fig. 1. Published documents for each term on arsenic and antimony adsorption and desorption from water.

In Fig. 1, we can also observe the gap between the adsorption and desorption studies. The desorption of arsenic or antimony has been reported approximately 5–6 times less often in academic publications than adsorption, even though desorption is an essential step of the treatment process. Antimony desorption may be even more relevant because the element is widely applied in industry and its recovery may be important because it is identified as being at critical levels of availability in some regions, such as the European continent (Cole-Hamilton, 2020).

Fig. S.1 presents the global distribution of publications on the terms "antimony AND desorption AND water" and "arsenic AND desorption AND water". China has the most publications in both terms, followed by the United States, which has a stronger presence in arsenic desorption. Among the top 20 countries ranking for publications on arsenic desorption we found the most affected countries by arsenic contamination in water: China, the U.S., India, Japan, Pakistan, Argentina, Brazil, Taiwan, Mexico, Vietnam, and Bangladesh.

China has been the largest antimony producer worldwide for 110 years, with >60 % of global production (in 2019), which is mainly associated with the major mined ore deposits located in the country (Herath et al., 2017; Nishad and Bhaskarapillai, 2021). Between 2006 and 2016, China released 1915.58 Gg of antimony into the biosphere, with a recycling rate of just 0.91 % in 2013 (Chu et al., 2019). This, together with the expanding scientific dominance of China, may help to explain the nation's interest in and leadership in antimony desorption research.

For both arsenic and antimony, three journals published more papers: Journal of Hazardous Materials, Chemosphere, and Science of the Total Environment. In terms of keywords associated to documents found for each expression, it's worth noting that "pH" was highly mentioned for both "desorption AND arsenic AND water" and "desorption AND antimony AND water". "Groundwater" and "iron" were among the top ten keywords associated to the documents published about "arsenic AND desorption AND water". This was expected, given iron's significant propensity to bind with arsenic, resulting in the incorporation of this element as the most common alteration of biosorbents to increase arsenic removal rates (Carneiro et al., 2021).

The research methodology of this systematic review consisted of searching the terms "arsenic AND desorption AND water" in the Scopus and Web of Science databases. The criteria for the selected articles included the presence of desorption/regeneration assays and the description of quantitative parameters, as summarized in Fig. S.2.

3. Adsorption of pnictogens

Antimony and arsenic are toxic elements that can be removed from water by similar low-cost treatment processes due to their chemical similarities; for example, good removal results by adsorption have been demonstrated.

When designing an adsorption system, the adsorbent type is not the only relevant aspect to be considered. The adsorption process can be dependent on the following factors: pH, pH_{zpc}, adsorbent dosage, temperature, pressure, surface area of the adsorbent, and presence of co-existing ions (Zaimee et al., 2021). Moreover, adsorption in continuous mode might also be affected by other parameters, such as flow rate, hydraulic retention time (HRT), and adsorbate initial concentration (Carneiro et al., 2021). Both Sb and As removal strategies can include the oxidation of the trivalent species, which are harder to adsorb, to the pentavalent species, which has greater affinity for most adsorbents.

Much research has been conducted on arsenic and antimony adsorption by different materials and under various conditions. The most frequent treatment for increasing the arsenic adsorption capacity

of adsorbent materials is iron incorporation, followed by the addition of other metals, such as aluminum and zirconium (Carneiro et al., 2021). The materials developed to adsorb arsenic usually exhibit affinity for antimony removal (Pintor et al., 2018; Pintor et al., 2020; Carneiro et al., 2022a; Vieira et al., 2017; Kavacık and Dölgen, 2023; Bacelo et al., 2020; Bacelo et al., 2022) due to the chemical characteristics shared by the elements. Nano adsorbents, such as carbon nanofibers, carbon nanotubes, and metal-organic frameworks (MOFs), have great potential for removing metalloids from contaminated effluents, however, their small diameter limits their application on a large scale. To overcome this issue, a hybrid aerogel with MOFs embedded in a cellulose nanocrystal matrix has been developed with a diameter of 2 cm (Zhang et al., 2023a). This aerogel was capable of adsorbing high quantities of Sb(V).

Because the resultant composites might inherit the properties of the parent materials while also displaying synergistic effects, the creation of composite adsorbents integrating two or more metal oxides may enhance their adsorption capacities (Zhang et al., 2023b). Not only have binary metal oxides reached significant adsorption capabilities, but so has biosorption (Carneiro et al., 2021). Biosorption has several advantages, such as the use of cheap abundant biomaterials, relatively low operational cost (Senthil Kumar and Ngueagni, 2022), and potential lower carbon emissions.

Arsenic and antimony can coexist in contaminated drinking water resources (Gan et al., 2023). There have been investigations on the effect of coexisting pnictogens (Pintor et al., 2021; Qiu et al., 2019) and the possibility of simultaneous As—Sb removal has been demonstrated (Pintor et al., 2022; Belozerova et al., 2022; Xu et al., 2022; Long et al., 2022). Lately, studies have found removal capacities of adsorption systems operating in continuous mode in the range of 4 to 30 mg g^{-1} of arsenic (Carneiro et al., 2022a; Saldaña-Robles et al., 2018; Ociński and Mazur, 2020) and 6 to 31 mg g^{-1} (Bacelo et al., 2022; Dabbagh et al., 2019; Zhu et al., 2021; Iqbal et al., 2013) of antimony. Fixed-bed columns operating with both elements have removed As and Sb under World Health Organization drinking water guidelines of 10 μgL^{-1} and 20 μgL^{-1}, respectively (Qiu et al., 2019; Lu et al., 2015).

Adsorption mechanisms include surface precipitation, physical adsorption, ion exchange, electrostatic attraction, and functional group complexation (Masindi et al., 2022). The type of interaction between the adsorbate and adsorbent can vary with the type of adsorbent and the element species. The Langmuir and Freundlich equilibrium models, which describe monolayer adsorption onto a homogeneous surface and chemisorption on a heterogeneous surface, respectively, are the most often used models for characterizing As (Yeo et al., 2021) and Sb adsorption (Long et al., 2020a; Peng et al., 2023).

4. Desorption parameters

Desorption can be viewed as the opposite of the adsorption process, in which adsorbates are released from the adsorbent surface either by substitution for an ion with a strong affinity for the saturated adsorbent or through chemical interactions with the eluent (Michael et al., 2018). Fig. S.3 illustrates how the adsorption/desorption process of arsenic/antimony takes place.

Eluents for As or Sb are commonly of three types: bases, acids or complexing agents. The bases usually exchange the hydroxyl groups for the As and Sb in the oxyanions forms; the acids usually dissolve the chemical interaction with protonic sites in the adsorbent; and the complexing agents will remove the adsorbate from the adsorbent by complexation. The optimal eluent is chosen by balancing i) desorption efficiency, ii) regeneration capacity of the adsorbent under treatment, and iii) toxicity and disposal of the eluting solution. Stronger eluent concentrations are usually associated to a higher desorption efficiency, however with a increased risk of damaging the adsorbent. Complexing agents are usually associated with a lower desorption efficiency and higher cost.

The desorption performance may be assessed by quantifying the desorption capacity, q_d (mg g^{-1}), and the desorption efficiency, d_e (%). The following equations can be used to calculate q_d and d_e.

In batch mode (Patel, 2021):

$$q_d = \frac{V^*C}{m}$$

where V is the solution volume (L), C *is* the concentration of adsorbate in the eluent after contacting the adsorbent (mg L^{-1}), and m is the mass of adsorbent (g).

In continuous mode:

$$q_d = \frac{adsorbate\ mass_{out}}{adsorbent\ mass}$$

where $adsorbate\ mass_{out}$ is the eluted mass of the adsorbate in the solution (mg), and *adsorbent mass* is the adsorbent mass in the bed (g).

The desorption efficiency can be defined for both modes as follows:

$$d_e = \frac{adsorbate\ mass_{out}}{adsorbate\ mass_{in}} \times 100$$

where $adsorbate\ mass_{in}$ is the mass of arsenic retained in the saturated adsorbent in the previous adsorption cycle.

The regeneration process can cause a decrease in the adsorption capacity of the adsorbent (q_{loss}), which can be calculated by the expression:

$$q_{loss}(\%) = \left(1 - \frac{q_r}{q_0}\right) \times 100$$

where q_r is the adsorption capacity after regeneration (mg g^{-1}) and q_0 is the initial adsorption capacity of the fresh adsorbent (mg g^{-1}).

The pH, time of contact or retention time, flow rate, eluent type, concentration of desorbing agent in solution, surface characteristics of the adsorbent, surface coverage, and coexisting ions all influence desorption efficiency, d_e (Carneiro et al., 2021; Tuutijärvi et al., 2012). Compared with fresh adsorbents, regenerated adsorbents commonly suffer a reduction in the adsorption parameters, such as adsorption capacity and breakthrough time, compared with the fresh adsorbent. This difference may be due to the degradation of the adsorbent or the presence of undesorbed arsenic/antimony. An increase in the mass transfer zone after adsorption-desorption cycles (Carneiro et al., 2022b) and an increase in arsenic adsorption capacity after 2 to 6 cycles were observed in the literature (Ociński and Mazur, 2020), which might be justified by the desorption of the remaining adsorbate from the previous cycles.

5. Desorption mechanism

Desorption equilibrium and kinetics can be represented by the same theoretical models of adsorption equilibrium (e.g. Langmuir (1918), Freundlich (1907)) and kinetics (e.g. pseudo-first-order, pseudo-second-order, Elovich and Larionov (1962)), yet this does not indicate that adsorption kinetics and mechanism are the same as for desorption (Ghosh et al., 2004). The adsorption and desorption curves are similar in batch mode; however, in continuous mode, the adsorption and desorption profiles are different, as shown in Fig. S.4. The graph from adsorption in continuous mode (Fig. S.4.c) was made using C/C_o values, which is more usual, but using mg L^{-1} experimental values on y-axis will result in the same shape.

Adsorption curves in continuous mode, also known as breakthrough curves, are "s"-shaped, and a range of models can be fitted to the experimental data, such as the Yan model (Yan et al., 2001), the Thomas model (Thomas, 1944), and the Yoon-Nelson model (Yoon and Nelson, 1984). Desorption curves are shaped like a half-bell curve, and no theoretical models currently exist to be applied for describing them.

The study of desorption kinetics is important to predict the possible leaching of pollutants from the spent adsorbent media. Slow desorption

kinetics may prevent equilibria from occurring with short elution times (Ghosh et al., 2004), which could reduce desorption efficiency in column mode and, as a result, the adsorption capacity of the material in subsequent cycles, thereby affecting its potential for reuse.

Arsenic desorption from different adsorbents using 0.1 M NaOH showed similar kinetics, with a rapid phase lasting approximately 4 h, followed by a slower phase lasting 24 h before reaching equilibrium (Carneiro et al., 2022b; Wang et al., 2016; He et al., 2018). Antimony desorption from rapeseed straw biochar was time-dependent, and biochar that had been coated with Mn was more stable than that without this element (Jia et al., 2020). Table S.1 shows the As/Sb desorption kinetics parameters for different adsorbents.

6. Desorption of arsenic

The desorption of arsenic and the regeneration performance of different types of adsorbents reported in the literature are summarized in Table 1. The adsorbent types were categorized into four groups: biochar and (modified) biosorbents, nanomaterials, commercial adsorbents, and others.

The biochar and modified biosorbents could be regenerated to remove arsenic for many cycles. For some biosorbents, such as green algae, the arsenic removal efficiency stayed above 90 % after 10 cycles (Tuzen et al., 2009). Most of the bio-based materials could be reused for 3–5 cycles with an adsorption capacity loss of about 10–40 %. Nanomaterials were reused for around six adsorption-desorption cycles, during which the adsorption loss ranged from 5 to 86 %. Commercial adsorbents achieved the lowest average reduction in adsorption capacity of around 6 %. This could be due to previous optimization of the products before they were released into the market.

In desorption experiments, As(V) was studied twice as much as As (III). In terms of desorption efficiency, different outcomes were reported for the two species, depending on the type of adsorbent used; it is more common to suffer higher loss of As(V) than As(III) adsorption capacity. After five adsorption-desorption cycles, functionalized sugarcane bagasse showed a 14 % reduction in As(III) adsorption capacity, whereas the reduction in As(V) adsorption capacity was 22 % (Gupta et al., 2015). Similar findings were observed for Fe(III) - biomass of *Staphylococcus xylosus* (Aryal et al., 2010), although Ce—Ti hybrid oxide, after five adsorption-desorption cycles, had lower arsenite adsorption capacity than arsenate (Li et al., 2010).

6.1. Analysis of desorption efficiency by type of eluent

Fig. 2 shows an overview of the eluents applied for the arsenic desorption studies presented in Table 1. The most common types of chemical eluents used to regenerate adsorbents were bases and acids, more specifically NaOH and HCl, respectively. Nevertheless, many salts were tested for arsenic removal because they are less aggressive toward material structures. A mixture of chemicals is also common practice for metal desorption (Lee et al., 2017; Chaudhary and Farrell, 2015).

6.1.1. Bases

Sodium hydroxide was the most explored eluent in the regeneration of arsenic-loaded adsorbents. Fig. 3 shows the desorption efficiency of NaOH by the type of adsorbent. We can observe that 0.1 M was the most applied concentration (with a pH close to 13 (Carneiro et al., 2022b)), mainly on biochar and (modified) biosorbents, which can be more sensitive to high pH solutions. The efficiency of NaOH in removing As from these materials varied widely, but for nanomaterials and other adsorbents, the desorption efficiency of NaOH ranged between about 70 and 100 %.

The increase in NaOH concentration was not strictly related to the increase in desorption efficiency. Some studies with varying ranges of NaOH concentrations found an optimal concentration of 0.1 M to achieve the highest arsenic desorption (Carneiro et al., 2022b; Asadi Haris et al., 2023). An optimal concentration of 2 %, between 1 % and 6 %, has also been reported (Chen et al., 2015). The higher performance of NaOH may be related to the repulsion of the adsorbent surface and the more negatively charged arsenate form AsO_4^{3-} at pH values above 11.5 (Ungureanu et al., 2015). For iron-based adsorbents, NaOH can be even more efficient due to the higher affinity of OH^- to form a bond with Fe^{3+} compared to AsO_4^{3-} (Tuutijärvi et al., 2012).

6.1.2. Acids

The most common acid eluent applied for arsenic desorption is HCl. The application of 0.09 M HCl to desorb both inorganic arsenic species from the Fe(III) - biomass of *Staphylococcus xylosus* was highly efficient in terms of the desorption rate (Aryal et al., 2010). After consecutive adsorption-desorption cycles, the adsorbent exhibited a decrease in adsorption capacity for both arsenate and arsenite, but the reduction in As(V) capacity was greater. A weaker acid solution of HCl 0.01 M was applied to regenerate orange peel biosorbents for three cycles (Abid et al., 2016). A greater reduction in the adsorption capacity of arsenate was observed for natural orange peel (NOP) than for charred orange peel (COP). A more successful acid desorption process was reported for Zinc-impregnated biochar (*Z*-LBC) using 2.5 % HCl, in which the adsorbent could pass through four regeneration cycles with only a slight loss in As (V) removal capacity (Park et al., 2021).

HNO_3 0.1 M was tested for arsenic elution from iron-coated cork granulates (ICG), but the desorption efficiency was found to be only 34 % (Carneiro et al., 2022b). Moreover, the desorbing agent caused high leaching of the iron present in the adsorbent. Many other adsorbents have been reported to suffer the same effect after desorption in acidic solutions (Yeo et al., 2022b; Ghimire et al., 2002). The hindrance in the application of acid eluents is sometimes the degradation of the adsorbent; thus, weaker acids, such as organic acids (Zhang et al., 2021), can be less aggressive, although with lower desorption rates. The iron-based adsorbents may need to reload the iron coating after desorption and before the next adsorption cycle (Yeo et al., 2022b). Performing a reloading may result in a reduction in the adsorbents's removal capacity, making it more advantageous to simply use a fresh adsorbent.

6.1.3. Salts and others

The desorption of arsenic was also reported in the literature using salts such as NaCl, Na_2CO_3, $NaNO_3$, Na_2SO_4, Na_2HPO_4 and $CaCl_2$. Arsenic desorption efficiencies of 100 % from PEI-coated bacterial biosorbent were achieved using 0.01 M Na_2SO_4 (Kim et al., 2019), and from activated carbons using 0.5 M $NaNO_3$ and 0.5 M NaCl (Di Natale et al., 2013). In comparison with other chemicals, NaCl has a lower acquisition cost, which makes it a very attractive choice (Di Natale et al., 2013).

In addition to bases, acids and salts, the complexing agent EDTA was considered for arsenic removal. However, EDTA had one of the lowest desorption efficiencies in a study using arsenic-loaded iron-coated cork granulates (Carneiro et al., 2022b). On the other hand, sodium acetate successfully removed arsenate from Zn-HypoGel sorbent, and the resin was regenerated for five adsorption-desorption cycles (Moffat et al., 2014).

7. Desorption of antimony

The effect of different chemical eluents on the performance of antimony desorption has also been explored in the literature. Table 2 summarizes the data reported in the literature for Sb(V) and Sb(III) desorption efficiencies as well as regeneration performance in batch mode for different types of adsorbents: biochar and (modified) biosorbents, nanomaterials, and others.

Most of the materials used in antimony adsorption-desorption cycles were nanomaterials. They often have greater adsorption capacities, which is advantageous for potential Sb recovery. On average, the antimony desorption efficiency reported in these studies was lower than that reported for arsenic.

Table 1
Desorption of arsenic and regeneration performance of adsorbents in batch mode.

Adsorbent	Species	Time (h)	Eluents	Desorption efficiency (%)	Cycles	Adsorp. capacity reduction	Ref.
Biochar and (modified) biosorbents							
Al(III) Kapok fibers	As(V)	1	0.01 M HCl	–	5	~33 %	(Yeo et al., 2022a)
Fe(III) modified Kapok fiber	As(V)	–	0.1 M HCl	–	4	~38 %	(Yeo et al., 2022b)
Charred orange peel (COP) Natural orange peel (NOP)	As(V)	1.5	0.01 M HCl	–	3	10 % 26 %	(Abid et al., 2016)
Fe(III) - biomass of *Staphylococcus xylosus*	As(III) As(V)	0.5 2	0.09 M HCl	100	5	~20 % ~40 %	(Aryal et al., 2010)
Garcinia cambogia plant	As(III)	0.5	0.05 M NaOH 0.1 M Na_2CO_3 0.2 M NaCl	~99	1	–	(Kamala et al., 2005)
Green alga (*U. cylindricum)*	As(III)	1	1 M HCl 1 M HNO_3	95 85	10	~2 %	(Tuzen et al., 2009)
HFO-treated sugarcane bagasse	As(V)	–	30 % HCl 1 M NaOH	17 54–85	1	–	(Pehlivan et al., 2013)
Thiol-functionalized sugarcane bagasse	As(III) As(V)	1	0.01 M HCl	–	5	14 % 22 %	(Gupta et al., 2015)
Iron-coated cork granulates (ICG)	As(V)	24	0.01 M NaOH 0.1 M NaOH 0.1 M KOH 0.1 M Na_2CO_3 0.1 M HNO_3 0.5 M Na_2HPO_4 0.5 M EDTA 0.5 M KNO_3	69 92 83 56 34 22 13 1.8	4 2 1 1 1 1 1 1	82 % 88 % - - - - - -	(Carneiro et al., 2022b)
Iron-impregnated biochar	As(V)	48	0.1 M NaOH	72–60	3	26–37 %	(He et al., 2018)
Polyethylenimine-coated bacterial biosorbent	As(V)	1	0.01 M NaCl 0.01 M Na_2SO_4 0.01 M NaOH	~85–55 ~100–95 100	3 3 3	- - 15 %	(Kim et al., 2019)
Water melon rind (WMR) Citric acid WMR Xanthated WMR	As(III)/As(V)	0.67	0.1 M NaOH	97–20 / 98–50 94–11 / 93–15 98–32 / 96–47	4	–	(Shakoor et al., 2018)
Zinc-impregnated lignin biochar (Z-LBC)	As(V)	–	2.5 % HCl	–	4	9 %	(Park et al., 2021)
Magnetic biochar from Kans grass	As(III) As(V)	14	0.5 M NaOH	68 89	1	–	(Baig et al., 2014)
Magnetic wheat straw	As(V)	3	0.1 M NaOH	–	10	>80 %	(Tian et al., 2011)
Hydrated ferric oxide biochar nanohybrids	As(III)	3 × 2	0.5 M NaOH	–	6	~10 %	(Zhu et al., 2022)
Magnetite-modified water hyacinth biochar	As(V)	12	0.1 M HCl	~80	4	49.2 %	(Zhang et al., 2016)
Ni/Mn-LDHs on pristine biochars (NMMB)	As(V)	48	0.1 M NaOH	81.7	3	2 %	(Wang et al., 2016)
Cross-linked alginate beads (CABs)	As(V)	–	0.3 M NaOH	~85	5	35 %	(Raval and Kumar, 2022)
Biochar (BC)/nZVZn	As(III) As(V)	0.67	0.2 M NaOH	77–31 78–43	3	–	(Masood ul Hasan et al., 2023)
Biochar/ Hydroxyapatite (BC/HA-alginate)	As(III) As(V)	0.67	0.2 M NaOH	88–30 64–25	3	–	(Masood ul Hasan et al., 2023)
Nanomaterials							
Chitosan graphene oxide-gadolinium oxide nanorods	As(V)	1	0.1 M NaOH	98–75	6	22 %	(Choi et al., 2020)
Cross-linked alginate beads impregnated with bilayer-oleic coated magnetite (CAB@BOFe)	As(V)	–	0.3 M NaOH	~11	5	8 %	(Raval and Kumar, 2022)
δ-MnO_2@Fe/Co-MOF-74 nanocomposite	As(III)	6	0.1 M NaOH	–	4	21.1 %	(Yang et al., 2021a)
Graphene nanoplatelets	As(III)	3	2.0 M NaOH 2.0 M KOH	68.35 81.07	1	–	(Nandi et al., 2021)
Magnetic γ-Fe_2O_3 nanoparticles	As(III) As(V)	3	1 M NaOH	–	6	61 % 40 %	(Lin et al., 2012)
Sol-gel maghemite nanoparticles	As(V)	48	1 M NaOH	>95	6	5–10 %	(Tuutijärvi et al., 2012)
Superparamagnetic iron oxide nanoparticles (SPIONs)	As(III)	–	0.1 M NaOH 0.1 M HCl	82 43	8 -	86 %	(Asadi Haris et al., 2023)
Electrospun polyethylenimine/polyvinyl chloride nanofiber sheets	As(V)	2	0.02 M NaOH	95	5	9 %	(Wang et al., 2023a)
Fe_3O_4@surfactants nanoparticles	As(V)	0.5	1 M NaOH	–	5	15 %	(Zhao et al., 2023)
Fe_3O_4 - polyurethane (PU) foam nanocomposite	As(V) + As (III)	–	0.1 M HCl + 0.1 M NaOH	90–70	5	28 %	(Tamaddoni Moghaddam et al., 2023)
La_2O_3-sawdust	As(III) As(V)	24	1 M HNO_3	100 93	1	0 %	(Setyono and Valiyaveettil, 2014)
ZrO_2-sawdust	As(III) As(V)	24	1 M NaOH	30 30	1	~50 %	(Setyono and Valiyaveettil, 2014)
Commercial adsorbents							

(*continued on next page*)

Table 1 (*continued*)

Adsorbent	Species	Time (h)	Eluents	Desorption efficiency (%)	Cycles	Adsorp. capacity reduction	Ref.
Activated carbon – Aquacarb 207 EA	As(V)	72	0.05–1 M NaCl 0.5 M $CaCl_2$ 0.5 M $NaNO_3$ 0.5 M NaOH	100 84 100 100	1	<7 %	(Di Natale et al., 2013)
ARM200 (VV)	As	24	6 % NaOH	87.2	1	–	(Chen et al., 2015)
Commercial maghemite	As(V)	48	1 M NaOH	>95	6	5 %	(Tuutijärvi et al., 2012)
E33-G	As	24	6 % NaOH	88.1	1	–	(Chen et al., 2015)
GFH	As	24	6 % NaOH	51.6	1	–	(Chen et al., 2015)
Lanthanum-modified iron oxide	As(V)	6	0.05 M NaOH 0.2 M NaOH 1 M NaOH	40.95 83.03 98.78–94.54	1 1 1–3	- - 6 %	(Dudek and Kołodyńska, 2022)
Nano-zero valent zinc (nZVZn)	As(III) As(V)	0.67	0.2 M NaOH	81–45 84–41	3	–	(Masood ul Hasan et al., 2023)
Others							
Amine-doped acrylic ion exchange fiber	As(V)	2	0.1 N HCl + 0.1 N NaOH	–	9	~17 %	(Lee et al., 2017)
Iron oxide coated geopolymer microspheres	As(III) As(V)	1	1 M NaOH	72 99	1	–	(Thakur and Armstrong, 2021)
Iron-oxide-coated natural rock (IOCNR)	As	6	1 M NaOH	95	1	~49 %	(Maji et al., 2011)
Hausmannite	As(V)	2	Citric acid pH 4 Citric acid pH 5 Citric acid pH 6	~40 ~60 ~67	1	–	(Barreto et al., 2020)
Hematite	As(V)	2	Citric acid pH 4 Citric acid pH 5 Citric acid pH 6	~17 ~46 ~71	1	–	(Barreto et al., 2020)
Ce-Ti hybrid oxide	As(III) As(V)	12	0.5 M NaOH	–	5	28 % 19 %	(Li et al., 2010)
Alginate beads-encapsulated SPIONs (SPIONs-Alg)	As(III)	–	0.1 M NaOH 0.1 M HCl	91 71	8 -	76 %	(Asadi Haris et al., 2023)
Magnetic iron oxide (MIO)	As(V)	–	1 M NaOH	~80 %	5	~2 %	(Zeng et al., 2024)

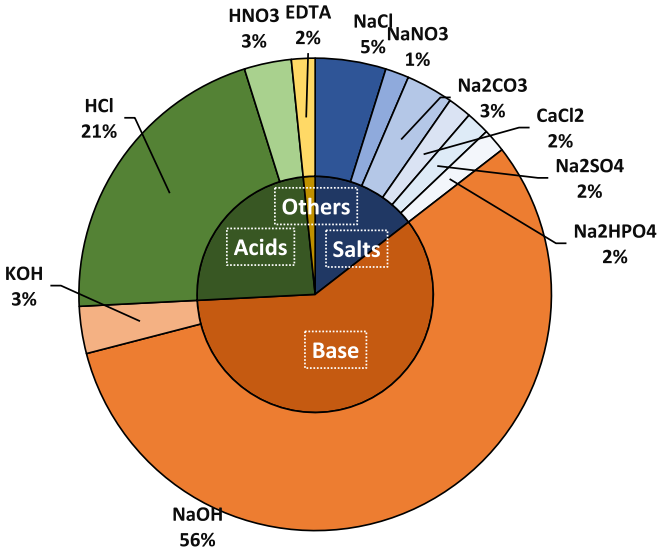

Fig. 2. Percentage of eluents used for arsenic desorption studies presented in Table 1.

Sb(V) desorption from MOF-Y and NH_2-MOF-Y was carried out with different eluents, and the best desorption efficiency was found in the following order: HCl > NaOH > Na_2CO_3 > NaCl > Na_2SO_4 > $NaNO_3$. However, strongly acidic conditions of HCl or strongly alkaline conditions of NaOH and Na_2CO_3 could damage the crystal structure of Y-based MOFs (Li et al., 2022), and the authors decided to explore adsorption/desorption cycles with the less aggressive eluent NaCl. After five consecutive adsorption-desorption cycles using NaCl, the remaining adsorption capacity was about 68 % of the initial one.

Antimonite desorption has been researched almost twice as much as antimonate's, and some studies have reported different desorption behavior for each species. For example, Sb(III)-loaded lanthanum-manganese binary oxide (L_1M_2BO) could be regenerated more effectively than the same adsorbent loaded with Sb(V) (Zhang et al., 2023b), but Sb(V) recovery rates from pine bark tannin resin were higher than that of Sb(III) (Bacelo et al., 2022).

All categories of adsorbent could be regenerated at high desorption rates and for many adsorption-desorption cycles. Treatment of adsorbents to improve their adsorption capacity might also improve their regenerability. Iron-biochar composites that went through a higher pyrolysis temperature demonstrated a higher Sb removal performance, even after five adsorption desorption cycles (Zhang et al., 2022).

7.1. Analysis of desorption efficiency by type of eluent

A summary of the eluents reported in the literature for Sb desorption is shown in Fig. 4. The most common eluents applied were HCl, NaOH, NaCl and EDTA. The best desorption efficiencies were achieved by acid solutions.

7.1.1. Bases

Approximately one third of the studies reported desorption of Sb using alkaline eluent, with NaOH being the only base used. The concentration of the alkaline solution varied from 0.1 to 1 M, with 0.5 M being the most common concentration. The regeneration of Zn-Fe-LDH loaded with As(V) and Sb(V) using 0.5 M NaOH released zinc in the solution (Lu et al., 2015). For metal-based adsorbents, elution can be associated with the leaching of the coating and compromise the performance of the adsorbent during future adsorption cycles. Overall, the desorption efficiency of NaOH was not high. However, NaOH has achieved good desorption efficiencies of 92.4 % and >80 % for some materials, such as carbon fibers decorated with ferric hydroxide (CF-Fe) (Simsek et al., 2018) and Fe—Mn binary oxides ($FMBO_3$) (Yang et al., 2018), respectively.

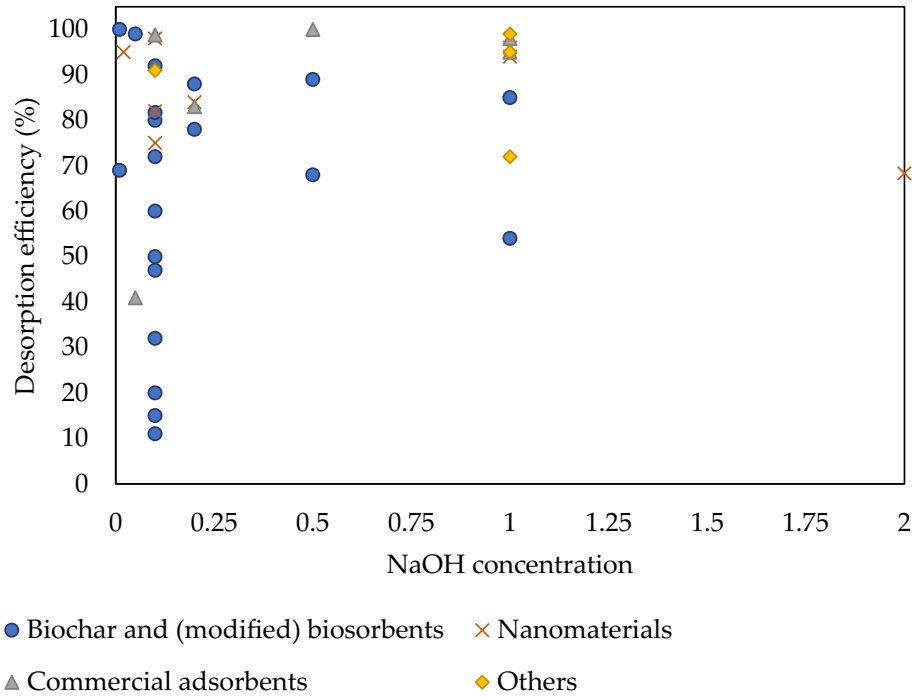

Fig. 3. Desorption efficiencies of arsenic-loaded adsorbents by NaOH at different concentrations reported in the literature.

7.1.2. Acids

Both inorganic and organic acids achieved high Sb desorption rates. However, HCl was the most frequently used eluent and had the highest desorption rates. These high desorption rates may be attributed to the formation of chloro-complexes (Runtti et al., 2023; Schweitzer and Pesterfield, 2010).

For arsenic desorption, NaOH solution was the most frequently used. As opposed to the behavior of Sb, which was best desorbed by acids, alkaline solutions were most effective on As. The differences between the As and Sb desorption mechanisms can be related to their molecular structure. Sb(V) is coordinated with oxygen in an octahedral geometry with a larger ionic radius (Pauling, 1933), while As(V) forms a lower spatial structure in a tetrahedral geometry (Simeonidis et al., 2017), leading to different adsorption (Pintor et al., 2020) and, consequently, desorption mechanisms.

Antimonite recovery from iron-modified chitosan was studied in batch mode using two types of eluent: HCl pH 3.5, and EDTA 0.01 M (Lapo et al., 2019). Three sorption-desorption cycles were conducted, and HCl was able to maintain a good recovery efficiency of 78–76 %, but EDTA desorbed less Sb(III), with a noticeable decay occurring between cycles, from 68 to 38 %.

The acid eluent was also applied for the desorption of Sb(III) from green bean husk (GBH) (Iqbal et al., 2013). The recovery efficiency achieved by HCl 0.1 M was very high and stable during seven adsorption-desorption cycles (98.8–90 %).

The plot of HCl desorption rates versus different concentrations (Fig. 5) showed that desorption is overall stable with increasing of acid concentration. Although HCl has shown good results for extracting Sb from saturated media, strong acid solutions can degrade adsorbents. The iron incorporated in adsorbents to increase adsorption capacity is likely to be eluted by acid solutions as reported in some studies (Carneiro et al., 2024; Zhang et al., 2022; Mei et al., 2021). Considering that the iron layer is the active binding site for Sb, the adsorbent loses its potential for use in subsequent adsorption-desorption cycles. Low HCl concentrations may be more suited to avoid adsorbent degradation if the HCl concentration has a minimal or no impact on Sb desorption efficiency.

7.1.3. Salts and complexing agents

Salts and complexing agents have been more often explored for Sb desorption than for As desorption. Even though EDTA was used as a desorbing agent in 9 % of the studies, very few of them reported desorption efficiency values. Graphene and graphene oxides could be regenerated with 0.1 M EDTA for seven or four cycles, respectively, with a small loss in adsorption capacity (Leng et al., 2012; Yang et al., 2015a). NaCl solution was also tested as an eluent in 9 % of the studies, and it was sometimes associated with other eluents. Desorption efficiency ranged from 15 to 87 %. Metal-Organic Frameworks (MOF) adsorbents could be regenerated with NaCl for five adsorption-desorption cycles with a loss of one-third of the Sb(V) removal efficiency (Li et al., 2022).

8. Batch vs continuous mode desorption

Although numerous investigations on As and Sb desorption have been performed (Sections 6 and 7), most of them were carried out in batch mode. Table 3 summarizes the performance of adsorbents regenerated in continuous mode reported in the literature. NaOH solutions of 0.005 M to 1 M were predominantly applied as eluents. Desorption tests using different eluents were carried out on ferric hydroxide-based adsorbents (Chaudhary and Farrell, 2015). The regeneration of media could be enhanced by adding NaCl to NaOH regenerating solutions. Arsenic desorption in continuous mode was more reported than that of antimony, with As(V) being the most studied species. Desorption efficiencies were high, perhaps as a result of previous batch mode operation that optimized the applied eluents and their corresponding concentrations. As expected, a decrease in the adsorption capacity of regenerated adsorbents was reported. Thus, investigating methods to minimize the loss of adsorption capacity is important for increasing the viability of desorption for practical usage.

The bed volumes needed for As desorption ranged from 100 to 178. For Sb, the values ranged from 10 to 4000; however, the highest value was obtained from an assay carried out with a very weak solution of 0.005 M NaOH.

Table 2
Desorption of antimony and regeneration performance of adsorbents in batch operation mode.

Adsorbent	Sb species	Time (h)	Eluents	Desorption efficiency (%)	Desorp. cycles	Adsorption capacity reduction	Ref.
Biochar and (modified) biosorbents							
Cyanobacteria *Microcystis*	Sb(V)	24	1 M EDTA	45.94	1	–	(Sun et al., 2014)
			1 M HCl	68.46			
			1 M Citric acid	51.45			
			1 M NaOH	30.55			
Green bean husk (GBH)	Sb(III)	1	0.1 M HCl	~98.8–90	7	~10 %	(Iqbal et al., 2013)
Iron-coated cork granulates (ICG)	Sb(V)	24	1 M HCl	81 ± 9	1	–	(Carneiro et al., 2024)
			0.1 M Ascorbic acid	66 ± 8			
			0.5 M Tartaric acid	29 ± 5			
			0.5 M NaOH	22 ± 4			
Iron-modified chitosan [Chifer(III)]	Sb(III)	24	HCl pH 3.5	78–76	3	11.4 %	(Lapo et al., 2019)
			0.01 M EDTA	68–38			
Marine algae *T. conoides*	Sb(III)	1	0.1 M HCl	>99	3	5 %	(Vijayaraghavan and Balasubramanian, 2011)
Marine algae *C. sericea*	Sb(III)	4	0.1 M NaOH	12	1	–	(Ungureanu et al., 2016)
			0.1 M HCl	17	1	–	
			0.5 M Na_2HPO_4	23	1	–	
			0.5 M NaCl	15–45	3	52 %	
$MnFe_2O_4$-MCM-41-SH	Sb(III)	4	0.1 M Citric acid	–	5	10.9 %	(Li and Fu, 2020)
Pine bark tannin resin	Sb(III)	48	0.1 M NaOH	27	1	–	(Bacelo et al., 2022)
	Sb(V)			49			
Tannins from *P. pinaster* bark	Sb(V)	12	0.5 M NaOH	69–28	2	–	(Bacelo et al., 2018)
Iron-biochar composites (FBC)	Sb(V)	–	0.1 M HCl	–	5	~50 %	(Zhang et al., 2022)
Amino-functionalized hydrothermal biochar (NMSH)	Sb(V)	–	0.5 M NaOH	–	4	9 %	(Deng et al., 2020)
Chitosan-loaded biochar	Sb(III)	–	0.5 M NaOH	–	3	19 %	(Chen et al., 2022)
Pristine biochar	Sb(III)	–	0.5 M NaOH	–	3	30 %	(Chen et al., 2022)
Lichen (*Physcia tribacia*) biomass	Sb(III)	0.5	0.5 M HCl	95	10	20 %	(Uluozlu et al., 2010)
			0.5 M HNO_3	78	1	–	
La-doped magnetic biochars	Sb(V)	12	0.5 M NaOH +5 M NaCl	–	6	30–44 %	(Wang et al., 2018)
Nanomaterials							
Carbon fibers decorated with ferric hydroxide (CF-Fe)	Sb(V)	–	3.0 M NaOH	96.6–76.5	7	4 %	(Simsek et al., 2018)
Ce-doped Fe_3O_4	Sb(III)	12	0.5 M NaOH	~100 %	3	~0–10 %	(Qi et al., 2017)
Chitosan-modified pumice (CTS-mPMC)	Sb(III)	0.5	0.5 M HCl	95–70	10	10 %	(Sari et al., 2017)
Graphene	Sb(III)	4	0.1 M EDTA	–	5	<20 %	(Leng et al., 2012)
Graphene oxide (GO)	Sb(III)	2	0.1 M EDTA	–	4	14.5 %	(Yang et al., 2015a)
Mercapto-functionalized hybrid sorbent	Sb(III)	4	3 M HCl	96.7 at 90 °C	1	–	(Fan et al., 2016)
				81.7 at 60 °C	1		
				56.4 at 25 °C	1		
NH_2-Fe_3O_4-NTA core-shell magnetic nanoparticle sorbents	Sb(III)	10	0.1 M EDTA	–	5	<20 %	(Hao et al., 2019)
Nano-Fe_3O_4 modified red mud	Sb(III)	4	0.5 M HCl	–	5	~90 %	(Peng et al., 2021)
			0.5 M NaOH			<40 %	
Polyamide-graphene (PAG) composite	Sb(III)	–	0.5 M HCl	95–80	6	–	(Saleh et al., 2017)
Si-doped Fe oxide composites ($SFOC_{10}$)	Sb(V)	8	0.5 M NaCl +0.5 M NaOH	~85–90	5	<15 %	(Yang et al., 2021b)
Y-tape molecular sieve adsorbent (NaY@Ce)	Sb(III)	12	1 M NaOH	–	4	35 %	(Yan et al., 2020)
Zirconium porphyrin-based MOF (PCN-222)	Sb(III)	5	0.5 M HCl	–	5	~20 %	(Guo et al., 2021)
MOF-Y	Sb(V)	24	NaCl	~85	5	32 %	(Li et al., 2022)
NH_2-MOF-Y	Sb(V)	24	NaCl	~87	5	32 %	(Li et al., 2022)
ZVI decorated carbon nanotubes (CNT – Fe(0))	Sb(III) Sb(V)	4	0.05 M HCl	75–65	5	7–19 %	(Mishra et al., 2016)
Superparamagnetic nanoparticles Fe@Mg-Al LDH	Sb(III)	–	Acetone	~60	1	–	(Motallebi et al., 2022)
			Ethanol	~66			
			Methanol	~57			
			HCl	~68			
			Acetone + HCl	~70			
			Ethanol + HCl	63			
			Methanol + HCl	~73			
Others							
Brucite	Sb(III)	2	1 M NaOH	28.2 %	1	–	(Runtti et al., 2023)
			1 M HCl	98.6 %			
Low-cost natural diatomite	Sb(III)	–	0.5 M HCl	–	10	3 %	(Sarı et al., 2010)
Hydromagnesite	Sb(III)	2	1 M NaOH	39.5 %	1	–	(Runtti et al., 2023)
			1 M HCl	98.7 %			

(*continued on next page*)

Table 2 (*continued*)

Adsorbent	Sb species	Time (h)	Eluents	Desorption efficiency (%)	Desorp. cycles	Adsorption capacity reduction	Ref.
Commercial Mg-rich mineral	Sb(III)	2	1 M NaOH 1 M HCl	12.9 % 88.7 %	1	–	(Runtti et al., 2023)
MIL-100(Fe)-NH_2	Sb(V)	12	0.1 M NaOH	–	3	~1 %	(Cheng et al., 2023)
Lanthanum-manganese binary oxide	Sb(III) Sb(V)	4	NaOH 2 % + NaCl 4 % + 20 % NaClO	–	5	20 % 28 %	(Zhang et al., 2023b)
Kaolinite	Sb(V)	12	0.1 M $MgSO_4$	80	1		(Xi et al., 2010)
Fe-Mn binary oxides ($FMBO_3$)	Sb(V)	8	1 M NaOH	>80	5	18 %	(Yang et al., 2018)

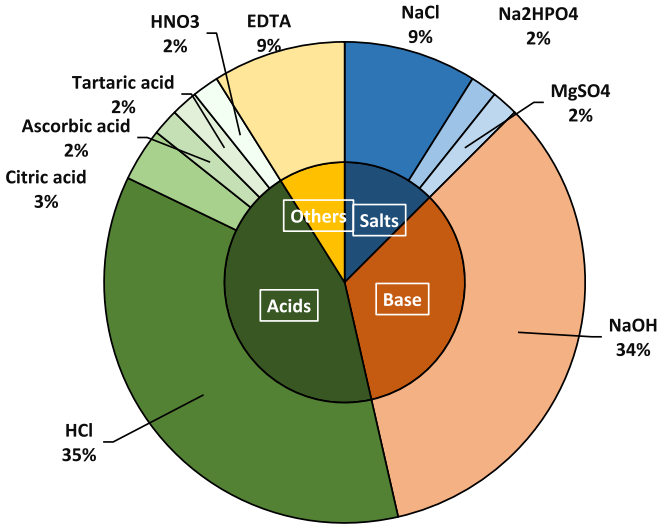

Fig. 4. Percentage of eluents used for antimony desorption studies presented in Table 2.

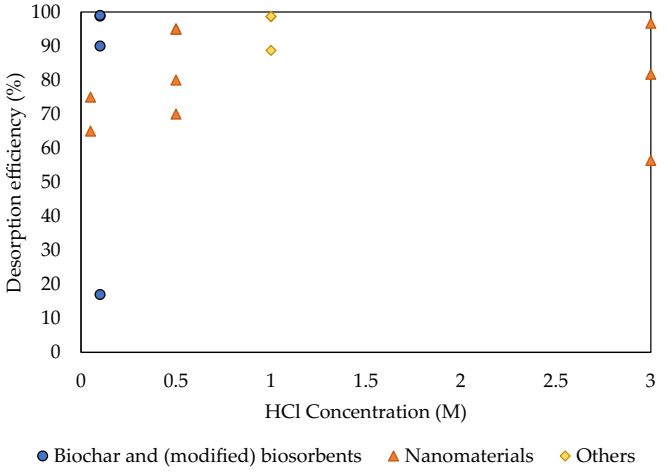

Fig. 5. Desorption efficiency of antimony-loaded adsorbents by HCl at different concentrations reported in the literature.

9. Regeneration and fate of spent adsorbent

One of the main concerns with employing adsorption for water treatment is what happens to the used adsorbent. Waste disposal is a serious issue in the majority of developing nations, and in many cases, the ecotoxic effects of its direct disposal impose a significant barrier to this procedure (Yadav et al., 2022).

It is common to incorporate metals to increase the material's adsorption capacity. However, to ensure regenerability and prevent metals from leaching into water, methods for making the coating durable and persistent are important (Thakur and Armstrong, 2021). When the coating is removed during desorption, recovering (or recycling) the adsorbent by treating it once again with the metal may be an interesting solution. Recycled Al(III)- and Fe(III)-modified kapok fiber (Yeo et al., 2022a; Yeo et al., 2022b) and iron-coated cork granulates (Carneiro et al., 2024) have improved adsorption capacities for arsenic and antimony, respectively.

The adsorbent, however, loses all of its adsorptive ability after a specific number of regeneration and reuse cycles and should finally be safely sent to a safe destination (Yadav et al., 2022). Some of these destinations can be immobilization, stabilization, and disposal. In developed countries, common disposal methods include landfilling and incineration; however, nations in economic development still lack the infrastructure to ensure that toxic waste is correctly disposed of, and much fewer safe procedures, such as dumping in backyards, ditches, and lowland areas, are carried out (Yadav et al., 2022). The European Union countries must account for the Directive (EU) 2018/850 of the European Parliament and of the Council of 30 May 2018 amending Directive 1999/31/EC on the landfill of waste. Even safer measures in developed countries can cause environmental problems, such as air pollution in the case of incineration (Yan et al., 2008). The mixing of biomass-derived spent adsorbents with coal was suggested as a viable option for energy generation in thermal plants, with possible metal recovery from incineration bottom ashes (Mondal and Garg, 2017). A life cycle assessment (LCA) compared the four most common strategies for As-rich Fe oxide water treatment residuals (WTRs) and revealed that landfilling had lower toxicity impacts compared to brick stabilization, mixture with organic waste, and open disposal (van Genuchten et al., 2022). It was concluded, however, that landfilling simply converts direct As emissions into an impending As toxicity issue for future generations.

The Toxicity Characteristic Leaching Procedure (TCLP) (SW, 1992) is a test that determines whether a waste material such as a spent adsorbent is hazardous or non-hazardous and, consequently, if it may be disposed of in hazardous waste landfills or municipal solid waste landfills. As disposal in a hazardous waste landfill may be 5 to 10 times more expensive than disposal in a municipal solid waste landfill, this categorization is crucial to the final cost of a given media-based treatment system (Impellitteri and Scheckel, 2006). The maximum level of arsenic in non-hazardous waste by TCLP is 5 mg L^{-1}. TCLP does not regulate antimony-loaded waste; however, other alternative toxicity tests, such as Soluble Threshold Limit Concentration (STLC) and Total Threshold Limit Concentration (TTLC), set thresholds of 15 mg L^{-1} and 500 mg kg^{-1} for antimony and 5 mg L^{-1} and 500 mg kg^{-1} for arsenic (DTSC, 2024).

10. Recovery and fate of desorbed solution

To recover an element from an exhausted bed, a large quantity of chemicals is consumed and a secondary effluent is generated (Hu et al., 2021). It was estimated that for arsenic removal from treatment systems, desorbed solution disposal might account for 95 % of the overall regeneration expenditures if there is not an onsite option for disposing of the regenerant wastewater at the water treatment plant (Sorg et al., 2017). The use of slow flow rates and high eluent concentrations has been suggested to reduce the amount of wastewater generated during

Table 3
Desorption of As and Sb and regeneration performance of adsorbents in continuous mode.

Adsorbent	Specie	Flow rate (mL/min)	Eluents	Desorption efficiency (%)	Desorp. cycles	Adsorp. capacity reduction	Bed volumes (BV)	Ref.
Polyethylenimine coated bacterial biosorbent	As(V)	16.7	0.1 M NaOH	99.6–99.8	5	–	–	(Kim et al., 2020)
Bark-based magnetic iron oxide particle (BMIOP)	As(III)	5	1 M NaOH	–	1	29.71 %	–	(Dhoble et al., 2022)
Fiban As5	As(V)	1.38	0.1 M NaOH	85	1	–	125	(Chaudhary and Farrell, 2015)
PAN-Fe	As(V)	1.38	0.1 M NaOH	78	1	–	125	(Chaudhary and Farrell, 2015)
FeOOH	As(V)	9.67	0.05 M NaOH	~90	1	~23 %	–	(Tresintsi et al., 2014)
Iron-coated cork granulates (ICG)	As(V)	5	0.01 M NaOH	74–100	5	53 %	112–178	(Carneiro et al., 2022b)
Iron oxide coated sponge (IOCSp)	As(III) As(V)	0.15 m/h	0.3 M NaOH	–	1	9 % 10 %	100 118	(Nguyen et al., 2010)
Iron (oxyhydr)oxide /CNT filters	Sb(III)	1.5	0.005 M NaOH	–	4	27.5 %	–	(Liu et al., 2019)
Quartz sand coated with Fe3O4 and graphene oxide (QFGO)	Sb(III)	10	0.1 M EDTA	–	2	–	~10	(Yang et al., 2015b)
Iron-coated cork granulates	Sb(V)	5	0.1 M ascorbic acid	88	1	82.5 %	~35	(Carneiro et al., 2024)

the regeneration process (Chaudhary and Farrell, 2015).

Very few studies have provided deep investigation on a feasible alternative destination for the metal-loaded solutions. Precipitation of Sb from the solution has been explored, through the addition of Na_2S to an antimony-high-concentrated effluent from desorption (Biswas et al., 2009). More than 98 % of the Sb(III) was precipitated and segregated from the solution, which also contained the iron leached from the adsorbent.

More recently, a study explored the secondary use of an antimony desorbing solution by applying it in the production of polyethylene terephthalate (PET) (Liang et al., 2022). KOH glycol solution was used as a desorbing agent for the Sb(III) saturated adsorbent, and the eluent solution was added to terephthalic acid to produce PET. In addition to the use of Sb-loaded eluent, the study investigated a final application to the saturated adsorbent by converting it into a catalyst for the reduction of nitroarenes.

Antimony recovery is a relevant field of research due to its strong role in industry and limited availability in the future. However, few antimony recovery experiments from adsorption/desorption processes have been reported, and the antimony recovery rates are still lower than those of arsenic.

A UV/sulfite advanced reduction method was proposed to remove arsenic oxyanions from water in the form of elemental arsenic (Wang et al., 2022). The suggested method might prevent the production of hazardous waste loaded with arsenic in addition to recovering arsenic.

The recovery of arsenic and alkali products from antimony smelting residues was carried out using a novel approach (Long et al., 2020b). The process, composed of eight steps, was based on the application of CO_2 and H_2SO_4, achieving an overall 80.6 % arsenic recovery efficiency. New methods are urgently needed to recover As from WTRs, convert it into valuable compounds, and reduce stored As toxicity and As emissions (van Genuchten et al., 2022). Arsenic recovery on a large scale is not yet recommended since this process is still not economically feasible and has limited applications (Mondal and Garg, 2017). Nevertheless, arsenic recovery might be feasible in the future because it is at risk of supply, according to the European Commission's list of Critical Raw Materials (European et al., 2023; Wang et al., 2023b).

Table 4 summarizes the possible fates of spent adsorbent and desorbed solution as discussed in Sections 9 and 10, respectively.

Table 4
Fate of wastes from As and Sb desorption process.

Fate of spent adsorbent	Fate of desorbed solution
• Regeneration of the adsorbent by recoating, reactivation or reloading.	• Precipitation of As/Sb from the solution (Biswas et al., 2009; Yang et al., 2024).
• Incorporation into composites used for construction, such as ceramic materials (Verbinnen et al., 2015; Rathore and Mondal, 2017) and cement (Tresintsi et al., 2014; Sarmah et al., 2019).	• Sb desorbing solution reuse by applying it in the production of polyethylene terephthalate (PET) (Liang et al., 2022).
• Mixing of biomass-derived spent adsorbents with coal for energy generation in thermal plants (Mondal and Garg, 2017).	• UV/sulfite advanced reduction method to remove arsenic oxyanions from water in the form of elemental arsenic (Wang et al., 2022).
• Non-hazardous waste management for TCLP results below 5 mg L^{-1}, e.g., non-hazardous landfill.	• Application of CO_2 and H_2SO_4 for arsenic recovery from antimony smelting residues (Long et al., 2020b).
• Hazardous waste management for TCLP results above 5 mg L^{-1}, e.g., hazardous landfill and incineration.	• Metal recovery from incineration bottom ashes (Mondal and Garg, 2017).
	• Hazardous waste management, e.g., hazardous landfill or incineration.

11. Challenges

i) Data on arsenic research are more available than Sb ones because of previous research efforts to understand and manage large-scale and long-term As environmental pollution concerns (Wilson et al., 2010). This reflects the higher number of publications on arsenic desorption than on Sb desorption. Nevertheless, there is a high demand for research on antimony desorption and recovery due to its limited availability in the future (Cole-Hamilton, 2020) and relevance in a variety of industrial applications.

ii) Most adsorption-desorption experiments reported in the literature were carried out in batch mode, even though real-scale operations in industry usually apply continuous flow mode. Pilot tests are the most costly but crucial for scaling novel adsorbents.

iii) Metal incorporation into adsorbents is important for increasing the adsorption capacity; however, desorption of metalloids can elute the metal coating and compromise the regeneration of the adsorbent for use in further adsorption cycles.

iv) More environmentally friendly materials are being produced for arsenic adsorption than for antimony adsorption. Because of the increased industrial value of antimony, more complex materials are being developed targeting Sb. The commercial applicability of an adsorbent should be determined not only by successful pilot-scale studies and adsorption/desorption feasibility but also by life cycle assessments to analyze the environmental impacts of these materials and whether the gains in adsorption capacity compensate for the environmental impact of production, operation, and disposal.

v) The proper disposal of spent media is a critical environmental concern in the water treatment sector. Finding the end destination for these materials, with a focus on overall environmental benefits, requires careful consideration of numerous factors. Therefore, further research in this field is needed. Meanwhile, a well-maintained landfill remains the most attractive option for the disposal of spent adsorbents after stabilization (Yadav et al., 2022).

vi) TCLP is the standard test for assessing a material's leachability and toxicity. On the other hand, it has been claimed to have many flaws and to underestimate leachability and, as a result, toxicity (Ghosh et al., 2004). Therefore, leachability studies of saturated adsorbents should be performed under a variety of experimental conditions to evaluate the stability of new adsorbents (Bai et al., 2022).

12. Final remarks

The desorption of arsenic and antimony is an important step in their cost-effective removal from water. The literature data show that the desorption of arsenic has been investigated more than antimony desorption. This difference might be related to the more well-known effect of arsenic on human health. A combination of factors, such as a decrease in Sb availability in the future and its higher economic value, might encourage Sb desorption/recovery studies. Therefore, antimony adsorption/desorption in aqueous solution might be an emerging field of study.

NaOH and HCl are the most often employed desorbing agents for the release of arsenic and antimony, respectively, from saturated adsorbents. Overall, lower desorption efficiencies were achieved for antimony than for arsenic. This approach might be a sensitive topic when it comes to recovering Sb from desorbing solutions and disposing of toxic media. Understanding the mechanisms and factors affecting arsenic and antimony desorption can help in the development of more effective adsorbents.

Moreover, further studies should be conducted to optimize the separation/recovery process of arsenic and antimony from the desorbed solution. Artificial intelligence is being used to create more reliable models for operational parameter prediction and process optimization, which might increase the viability of desorption.

Finally, finding an economic and environmental balance in the development of new adsorbents and alternative destinations for spent adsorbents at the end-of-life is among the most important tasks in the field for the following years.

Funding

This work was supported by national funds through FCT/MCTES (PIDDAC): LSRE-LCM, UIDB/50020/2020 (DOI:10.54499/UIDB/50020/2020) and UIDP/50020/2020 (DOI:10.54499/UIDP/50020/2020); and ALiCE, LA/P/0045/2020 (DOI:10.54499/LA/P/0045/2020). A. Pintor acknowledges her Junior Researcher contract CEECIND/01485/2017 (DOI 10.54499/CEECIND/01485/2017/CP1399/CT0012) by FCT. M. Carneiro acknowledges her Ph.D. scholarship by FCT [DOI 10.54499/2020.07233.BD].

CRediT authorship contribution statement

Mariko A. Carneiro: Conceptualization, Methodology, Formal analysis, Investigation, Data curation, Writing - Original Draft, Visualization. **Ariana M.A. Pintor:** Writing – review & editing, Validation, Supervision, Project administration, Investigation, Conceptualization. **Rui A.R. Boaventura:** Writing – review & editing, Resources, Funding acquisition. **Cidália M.S. Botelho:** Writing – review & editing, Supervision, Resources, Funding acquisition.

Declaration of competing interest

The authors declare that they have no known competing financial interests or personal relationships that could have appeared to influence the work reported in this paper.

Data availability

Data will be made available on request.

Acknowledgements

Some figures in this manuscript were created with BioRender.com.

Appendix A. Supplementary data

Supplementary data to this article can be found online at https://doi.org/10.1016/j.scitotenv.2024.172602.

References

(MOH), M.o.H.o.t.P.s.R.o.C, 2006. Chinese National Standards GB 3838-2002: sanitary standards for drinking water quality. In: S.A.o.C. (SAC) (Ed.), China Water Risk:: Hongkong, China.

Abid, M., et al., 2016. Arsenic(V) biosorption by charred orange peel in aqueous environments. Int. J. Phytoremediation 18 (5), 442–449. https://doi.org/10.1080/15226514.2015.1109604.

Alka, S., et al., 2021. Arsenic removal technologies and future trends: a mini review. J. Clean. Prod. 278, 123805. https://doi.org/10.1016/j.jclepro.2020.123805.

Aryal, M., Ziagova, M., Liakopoulou-Kyriakides, M., 2010. Study on arsenic biosorption using Fe(III)-treated biomass of Staphylococcus xylosus. Chem. Eng. J. 162 (1), 178–185. https://doi.org/10.1016/j.cej.2010.05.026.

Asadi Haris, S., et al., 2023. Alginate coated superparamagnetic iron oxide nanoparticles as nanocomposite adsorbents for arsenic removal from aqueous solutions. Sep. Purif. Technol. 310, 123193. https://doi.org/10.1016/j.seppur.2023.123193.

Asere, T.G., Stevens, C.V., Du Laing, G., 2019. Use of (modified) natural adsorbents for arsenic remediation: a review. Sci. Total Environ. 676, 706–720. https://doi.org/10.1016/j.scitotenv.2019.04.237.

Bacelo, H., et al., 2018. Recovery and valorization of tannins from a forest waste as an adsorbent for antimony uptake. J. Clean. Prod. 198, 1324–1335. https://doi.org/10.1016/j.jclepro.2018.07.086.

Bacelo, H., Santos, S.C.R., Botelho, C.M.S., 2020. Removal of arsenic from water by an iron-loaded resin prepared from Pinus pinaster bark tannins. Euro-Mediterr. J. Environ. Integr. 5 (3) https://doi.org/10.1007/s41207-020-00190-y.

Bacelo, H., et al., 2022. Antimony removal from water by pine bark tannin resin: batch and fixed-bed adsorption. J. Environ. Manage. 302, 114100. https://doi.org/10.1016/j.jenvman.2021.114100.

Bai, Y., et al., 2022. Application of iron-based materials for removal of antimony and arsenic from water: sorption properties and mechanism insights. Chem. Eng. J. 431, 134143. https://doi.org/10.1016/j.cej.2021.134143.

Baig, S.A., et al., 2014. Effect of synthesis methods on magnetic Kans grass biochar for enhanced As(III, V) adsorption from aqueous solutions. Biomass Bioenergy 71, 299–310. https://doi.org/10.1016/j.biombioe.2014.09.027.

Barreto, M.S.C., Elzinga, E.J., Alleoni, L.R.F., 2020. Hausmannite as potential As(V) filter. Macroscopic and spectroscopic study of As(V) adsorption and desorption by citric acid. Environ. Pollut. 262, 114196. https://doi.org/10.1016/j.envpol.2020.114196.

Baskar, A.V., et al., 2022. Recovery, regeneration and sustainable management of spent adsorbents from wastewater treatment streams: a review. Sci. Total Environ. 822, 153555. https://doi.org/10.1016/j.scitotenv.2022.153555.

Belozerova, A.A., et al., 2022. Sorption recovery of arsenic (III) and antimony (III) from solutions using MnO2/C nanocomposite. AIP Conf. Proc. https://doi.org/10.1063/5.0088904.

Biswas, B.K., et al., 2009. Effective removal and recovery of antimony using metal-loaded saponified orange waste. J. Hazard. Mater. 172 (2), 721–728. https://doi.org/10.1016/j.jhazmat.2009.07.055.

Bolan, N., et al., 2022. Antimony contamination and its risk management in complex environmental settings: a review. Environ. Int. 158, 106908. https://doi.org/10.1016/j.envint.2021.106908.
Carneiro, M.A., et al., 2021. Current trends of arsenic adsorption in continuous mode: literature review and future perspectives. Sustainability 13 (3), 1186.
Carneiro, M.A., et al., 2022a. Efficient removal of arsenic from aqueous solution by continuous adsorption onto iron-coated cork granulates. J. Hazard. Mater. 128657. https://doi.org/10.1016/j.jhazmat.2022.128657.
Carneiro, M.A., et al., 2022b. Multi-cycle regeneration of arsenic-loaded iron-coated cork granulates for water treatment. J. Water Process Eng. 50, 103291. https://doi.org/10.1016/j.jwpe.2022.103291.
Carneiro, M.A., T.A.S., Teixeira, P.J.S., Pintor, A.M.A., Boaventura, R.A.R., Botelho, C.M. S., 2024. New insights on antimony removal and recovery from water and wastewater using iron-coated cork granulates: desorption on batch and fixed-bed column systems. Chem. Eng. Sci. (under review).
Chaudhary, B.K., Farrell, J., 2015. Understanding regeneration of arsenate-loaded ferric hydroxide-based adsorbents. Environ. Eng. Sci. 32 (4), 353–360. https://doi.org/10.1089/ees.2014.0453.
Chen, A.S.C., Sorg, T.J., Wang, L., 2015. Regeneration of iron-based adsorptive media used for removing arsenic from groundwater. Water Res. 77, 85–97. https://doi.org/10.1016/j.watres.2015.03.004.
Chen, H., et al., 2022. Enhanced sorption of trivalent antimony by chitosan-loaded biochar in aqueous solutions: characterization, performance and mechanisms. J. Hazard. Mater. 425, 127971. https://doi.org/10.1016/j.jhazmat.2021.127971.
Cheng, M., et al., 2023. Grafting amino groups to enhance the adsorption of antimonate by MIL-100(Fe) for from natural water: performance and mechanism. Chem. Eng. J. Adv. 14, 100458. https://doi.org/10.1016/j.ceja.2023.100458.
Cheng, M.S., et al., Review of recently used adsorbents for antimony removal from contaminated water. Environ. Sci. Pollut. Res.DOI:https://doi.org/10.1007/s11356-022-18653-w.
Choi, J.-S., et al., 2020. Fabrication of chitosan/graphene oxide-gadolinium nanorods as a novel nanocomposite for arsenic removal from aqueous solutions. J. Mol. Liq. 320, 114410. https://doi.org/10.1016/j.molliq.2020.114410.
Chu, J., Mao, J., He, M., 2019. Anthropogenic antimony flow analysis and evaluation in China. Sci. Total Environ. 683, 659–667. https://doi.org/10.1016/j.scitotenv.2019.05.293.
Cole-Hamilton, D., 2020. The role of chemists and chemical engineers in a sustainable world. Chem. Eur. J. 26 (9), 1894–1899. https://doi.org/10.1002/chem.201905748.
Dabbagh, R., Mirkamali, M.-s., Vafajoo, L., 2019. Removal of antimony metalloid from synthetic effluent using seaweed as a low-cost natural sorbent: adsorption on a fixed-bed column. J. Water Chem. Technol. 41 (1), 21–28. https://doi.org/10.3103/S1063455X19010041.
Deliyanni, E.A., et al., 2015. Activated carbons for the removal of heavy metal ions: a systematic review of recent literature focused on lead and arsenic ions. Open Chem. 13 (1), 699–708. https://doi.org/10.1515/chem-2015-0087.
Deng, R.-J., et al., 2017. The potential for the treatment of antimony-containing wastewater by iron-based adsorbents. Water 9 (10), 794.
Deng, J., et al., 2020. Different adsorption behaviors and mechanisms of a novel amino-functionalized hydrothermal biochar for hexavalent chromium and pentavalent antimony. Bioresour. Technol. 310, 123438. https://doi.org/10.1016/j.biortech.2020.123438.
Dhoble, R.M., et al., 2022. Arsenite removal from drinking water by bark-based magnetic iron oxide particle (BMIOP): a column study. Environ. Sci. Pollut. Res. https://doi.org/10.1007/s11356-022-19443-0.
Di Natale, F., Erto, A., Lancia, A., 2013. Desorption of arsenic from exhaust activated carbons used for water purification. J. Hazard. Mater. 260, 451–458. https://doi.org/10.1016/j.jhazmat.2013.05.055.
Dias, A.C., Fontes, M.P.F., 2020. Arsenic (V) removal from water using hydrotalcites as adsorbents: a critical review. Appl. Clay Sci. 191, 105615.
DTSC. D.o.T.S.C. Persistent and Bioaccumulative Toxic Substances. [23/01/2024]. Available from. https://dtsc.ca.gov/persistent-and-bioaccumulative-toxic-substances/.
Dudek, S., Kołodyńska, D., 2022. Arsenic(V) removal on the lanthanum-modified ion exchanger with quaternary ammonium groups based on iron oxide. J. Mol. Liq. 347, 117985. https://doi.org/10.1016/j.molliq.2021.117985.
Elovich, S.Y., Larionov, O.G., 1962. Theory of adsorption from nonelectrolyte solutions on solid adsorbents. Bull. Acad. Sci. USSR Div. Chem. Sci. 11 (2), 198–203. https://doi.org/10.1007/BF00908017.
EPA, 2002. E.P.A., National primary drinking water regulations: long term 1 enhanced surface water treatment rule. Final rule. Fed. Regist. 67 (9), 1811–1844.
European Union, C, 2020. Council directive 2020/2184 of 16 December 2020. Off. J. Eur. Commun. L. 62.
European, C., et al., 2023. Study on the critical raw materials for the EU 2023 – Final report. In: Publications Office of the European Union. https://doi.org/10.2873/725585.
Fan, H.-T., et al., 2016. Adsorption of antimony(III) from aqueous solution by mercapto-functionalized silica-supported organic–inorganic hybrid sorbent: mechanism insights. Chem. Eng. J. 286, 128–138. https://doi.org/10.1016/j.cej.2015.10.048.
Freundlich, H., 1907. Über die Adsorption in Lösungen. Z. Phys. Chem. 57U (1), 385–470. https://doi.org/10.1515/zpch-1907-5723.
Gagliano, E., et al., 2020. Removal of poly- and perfluoroalkyl substances (PFAS) from water by adsorption: role of PFAS chain length, effect of organic matter and challenges in adsorbent regeneration. Water Res. 171, 115381. https://doi.org/10.1016/j.watres.2019.115381.
Gallegos-Garcia, M., Ramírez-Muñiz, K., Song, S., 2012. Arsenic removal from water by adsorption using Iron oxide minerals as adsorbents: a review. Miner. Process. Extr. Metall. Rev. 33 (5), 301–315. https://doi.org/10.1080/08827508.2011.584219.
Gan, Y., et al., 2023. Antimony (Sb) pollution control by coagulation and membrane filtration in water/wastewater treatment: a comprehensive review. J. Hazard. Mater. 442, 130072. https://doi.org/10.1016/j.jhazmat.2022.130072.
Gebel, T., 1997. Arsenic and antimony: comparative approach on mechanistic toxicology. Chem. Biol. Interact. 107 (3), 131–144. https://doi.org/10.1016/S0009-2797(97)00087-2.
Ghimire, K.N., et al., 2002. Adsorptive removal of arsenic using orange juice residue. Sep. Sci. Technol. 37 (12), 2785–2799. https://doi.org/10.1081/SS-120005466.
Ghosh, A., Mukiibi, M., Ela, W., 2004. TCLP underestimates leaching of arsenic from solid residuals under landfill conditions. Environ. Sci. Technol. 38 (17), 4677–4682. https://doi.org/10.1021/es030707w.
Giles, D.E., et al., 2011. Iron and aluminium based adsorption strategies for removing arsenic from water. J. Environ. Manage. 92 (12), 3011–3022. https://doi.org/10.1016/j.jenvman.2011.07.018.
Guan, X.H., et al., 2012. Application of titanium dioxide in arsenic removal from water: a review. J. Hazard. Mater. 215, 1–16. https://doi.org/10.1016/j.jhazmat.2012.02.069.
Guo, X., et al., 2014. Adsorption of antimony onto iron oxyhydroxides: adsorption behavior and surface structure. J. Hazard. Mater. 276, 339–345. https://doi.org/10.1016/j.jhazmat.2014.05.025.
Guo, Y., et al., 2021. Investigation of antimony adsorption on a zirconium-porphyrin-based metal–organic framework. Dalton Trans. 50 (39), 13932–13942. https://doi.org/10.1039/D1DT01895G.
Gupta, A., Vidyarthi, S.R., Sankararamakrishnan, N., 2015. Concurrent removal of As(III) and As(V) using green low cost functionalized biosorbent – Saccharum officinarum bagasse. J. Environ. Chem. Eng. 3 (1), 113–121. https://doi.org/10.1016/j.jece.2014.11.023.
Habuda-Stanic, M., Nujic, M., 2015. Arsenic removal by nanoparticles: a review. Environ. Sci. Pollut. Res. 22 (11), 8094–8123. https://doi.org/10.1007/s11356-015-4307-z.
Hao, H., et al., 2019. Simultaneous cationic Cu (II)–anionic Sb (III) removal by NH2-Fe3O4-NTA core-shell magnetic nanoparticle sorbents synthesized via a facile one-pot approach. J. Hazard. Mater. 362, 246–257. https://doi.org/10.1016/j.jhazmat.2018.08.096.
He, R., et al., 2018. Synthesis and characterization of an iron-impregnated biochar for aqueous arsenic removal. Sci. Total Environ. 612, 1177–1186. https://doi.org/10.1016/j.scitotenv.2017.09.016.
Herath, I., Vithanage, M., Bundschuh, J., 2017. Antimony as a global dilemma: geochemistry, mobility, fate and transport. Environ. Pollut. 223, 545–559. https://doi.org/10.1016/j.envpol.2017.01.057.
Hu, X., et al., 2021. Recent advances in antimony removal using carbon-based nanomaterials: a review. Front. Environ. Sci. Eng. 16 (4), 48. https://doi.org/10.1007/s11783-021-1482-7.
Impellitteri, C.A., Scheckel, K.G., 2006. The distribution, solid-phase speciation, and desorption/dissolution of as in waste iron-based drinking water treatment residuals. Chemosphere 64 (6), 875–880. https://doi.org/10.1016/j.chemosphere.2006.02.001.
Iqbal, M., Saeed, A., Edyvean, R.G.J., 2013. Bioremoval of antimony(III) from contaminated water using several plant wastes: optimization of batch and dynamic flow conditions for sorption by green bean husk (Vigna radiata). Chem. Eng. J. 225, 192–201. https://doi.org/10.1016/j.cej.2013.03.079.
Jia, X., et al., 2020. The antimony sorption and transport mechanisms in removal experiment by Mn-coated biochar. Sci. Total Environ. 724, 138158. https://doi.org/10.1016/j.scitotenv.2020.138158.
Kamala, C.T., et al., 2005. Removal of arsenic(III) from aqueous solutions using fresh and immobilized plant biomass. Water Res. 39 (13), 2815–2826. https://doi.org/10.1016/j.watres.2005.04.059.
Kavacık, B., Dölgen, D., 2023. Arsenic and antimony removal by using thermal modified treatment plant sludge in a fixed bed column. J. Fac. Eng. Archit. Gazi Univ. 38 (1), 629–638. https://doi.org/10.17341/gazimmfd.1020632.
Kim, N., et al., 2019. Removal of anionic arsenate by a PEI-coated bacterial biosorbent prepared from fermentation biowaste. Chemosphere 226, 67–74. https://doi.org/10.1016/j.chemosphere.2019.03.113.
Kim, N., et al., 2020. New insight into continuous recirculation-process for treating arsenate using bacterial biosorbent. Bioresour. Technol. 316, 123961. https://doi.org/10.1016/j.biortech.2020.123961.
Langmuir, I., 1918. The adsorption of gases on plane surfaces of glass, mica and platinum. J. Am. Chem. Soc. 40 (9), 1361–1403. https://doi.org/10.1021/ja02242a004.
Lapo, B., et al., 2019. Antimony removal from water by a chitosan-iron(III)[ChiFer(III)] biocomposite. Polymers 11 (2). https://doi.org/10.3390/polym11020351.
Lata, S., Samadder, S., 2016. Removal of arsenic from water using nano adsorbents and challenges: a review. J. Environ. Manage. 166, 387–406.
Lata, S., Singh, P.K., Samadder, S.R., 2015. Regeneration of adsorbents and recovery of heavy metals: a review. Int. J. Environ. Sci. Technol. 12 (4), 1461–1478. https://doi.org/10.1007/s13762-014-0714-9.
Lee, C.-G., et al., 2017. Arsenic(V) removal using an amine-doped acrylic ion exchange fiber: kinetic, equilibrium, and regeneration studies. J. Hazard. Mater. 325, 223–229. https://doi.org/10.1016/j.jhazmat.2016.12.003.
Leng, Y., et al., 2012. Removal of antimony(III) from aqueous solution by graphene as an adsorbent. Chem. Eng. J. 211-212, 406–411. https://doi.org/10.1016/j.cej.2012.09.078.

Li, W., Fu, F., 2020. Incorporating MnFe2O4 onto the thiol-functionalized MCM-41 for effective capturing of Sb(III) in aqueous media. Microporous Mesoporous Mater. 298, 110060. https://doi.org/10.1016/j.micromeso.2020.110060.
Li, Z., et al., 2010. As(V) and as(III) removal from water by a Ce–Ti oxide adsorbent: behavior and mechanism. Chem. Eng. J. 161 (1), 106–113. https://doi.org/10.1016/j.cej.2010.04.039.
Li, J., et al., 2018. Antimony contamination, consequences and removal techniques: a review. Ecotoxicol. Environ. Saf. 156, 125–134. https://doi.org/10.1016/j.ecoenv.2018.03.024.
Li, Q., et al., 2022. Efficient removal of antimonate from water by yttrium-based metal-organic framework: adsorbent stability and adsorption mechanism investigation. Colloids Surf. A Physicochem. Eng. Asp. 633, 127877. https://doi.org/10.1016/j.colsurfa.2021.127877.
Liang, J., et al., 2022. Recovery of antimony using biological waste and stepwise resourcization as catalysts for both polyesterification and transfer hydrogenation. Colloids Surf. A Physicochem. Eng. Asp. 635, 128119. https://doi.org/10.1016/j.colsurfa.2021.128119.
Lin, S., Lu, D., Liu, Z., 2012. Removal of arsenic contaminants with magnetic γ-Fe2O3 nanoparticles. Chem. Eng. J. 211-212, 46–52. https://doi.org/10.1016/j.cej.2012.09.018.
Liu, Y., et al., 2019. Nanoscale iron (oxyhydr) oxide-modified carbon nanotube filter for rapid and effective Sb (III) removal. RSC Adv. 9 (32), 18196–18204.
Liu, B., et al., 2020. A review of functional sorbents for adsorptive removal of arsenic ions in aqueous systems. J. Hazard. Mater. 388, 121815. https://doi.org/10.1016/j.jhazmat.2019.121815.
Long, X., et al., 2020a. A review of removal technology for antimony in aqueous solution. J. Environ. Sci. 90, 189–204. https://doi.org/10.1016/j.jes.2019.12.008.
Long, H., et al., 2020b. Separation and recovery of arsenic and alkali products during the treatment of antimony smelting residues. Miner. Eng. 153, 106379. https://doi.org/10.1016/j.mineng.2020.106379.
Long, X., Wang, T., He, M., 2022. Simultaneous removal of antimony and arsenic by nano-TiO2-crosslinked chitosan (TA-chitosan) beads. Environ. Technol. 1–11. https://doi.org/10.1080/09593330.2022.2048084.
Lu, H., et al., 2015. Simultaneous removal of arsenate and antimonate in simulated and practical water samples by adsorption onto Zn/Fe layered double hydroxide. Chem. Eng. J. 276, 365–375. https://doi.org/10.1016/j.cej.2015.04.095.
Maia, L.C., Soares, L.C., Alves Gurgel, L.V., 2021. A review on the use of lignocellulosic materials for arsenic adsorption. J. Environ. Manage. 288, 112397. https://doi.org/10.1016/j.jenvman.2021.112397.
Maji, S.K., Kao, Y.H., Liu, C.W., 2011. Arsenic removal from real arsenic-bearing groundwater by adsorption on iron-oxide-coated natural rock (IOCNR). Desalination 280 (1), 72–79. https://doi.org/10.1016/j.desal.2011.06.048.
Masindi, V., et al., 2022. Challenges and avenues for acid mine drainage treatment, beneficiation, and valorisation in circular economy: a review. Ecol. Eng. 183, 106740. https://doi.org/10.1016/j.ecoleng.2022.106740.
Masood ul Hasan, I., et al., 2023. Biochar/nano-zerovalent zinc-based materials for arsenic removal from contaminated water. Int. J. Phytoremediation 25 (9), 1155–1164. https://doi.org/10.1080/15226514.2022.2140778.
Meez, E., et al., 2021. Activated carbons for arsenic removal from natural waters and wastewaters: a review. WATER 13 (21). https://doi.org/10.3390/w13212982.
Mei, Y., et al., 2021. Effect of Fe–N modification on the properties of biochars and their adsorption behavior on tetracycline removal from aqueous solution. Bioresour. Technol. 325, 124732. https://doi.org/10.1016/j.biortech.2021.124732.
Michael, F.M., et al., 2018. In: Shimpi, N.G. (Ed.), 2 - Surface Modification Techniques of Biodegradable and Biocompatible Polymers, in Biodegradable and Biocompatible Polymer Composites. Woodhead Publishing, pp. 33–54. https://doi.org/10.1016/B978-0-08-100970-3.00002-X.
Mishra, S., et al., 2016. Removal of antimonite (Sb(iii)) and antimonate (Sb(v)) using zerovalent iron decorated functionalized carbon nanotubes. RSC Adv. 6 (98), 95865–95878. https://doi.org/10.1039/C6RA18965B.
Moffat, C.D., et al., 2014. Molecular recognition and scavenging of arsenate from aqueous solution using dimetallic receptors. Chem. Eur. J. 20 (51), 17168–17177. https://doi.org/10.1002/chem.201404723.
Mondal, M.K., Garg, R., 2017. A comprehensive review on removal of arsenic using activated carbon prepared from easily available waste materials. Environ. Sci. Pollut. Res. 24 (15), 13295–13306. https://doi.org/10.1007/s11356-017-8842-7.
Motallebi, R., et al., 2022. Fabrication of superparamagnetic adsorbent based on layered double hydroxide as effective nanoadsorbent for removal of Sb (III) from water samples. IET Nanobiotechnol. 16 (2), 33–48. https://doi.org/10.1049/nbt2.12074.
Müller, V., et al., 2022. Increasing temperature and flooding enhance arsenic release and biotransformations in Swiss soils. Sci. Total Environ. 838, 156049. https://doi.org/10.1016/j.scitotenv.2022.156049.
Nandi, D., et al., 2021. Arsenic removal from water by graphene nanoplatelets prepared from nail waste: a physicochemical study of adsorption based on process optimization, kinetics, isotherm and thermodynamics. Environ. Nanotechnol. Monit. Manag. 16, 100564. https://doi.org/10.1016/j.enmm.2021.100564.
Nguyen, T.V., et al., 2010. Arsenic removal by iron oxide coated sponge: experimental performance and mathematical models. J. Hazard. Mater. 182 (1), 723–729. https://doi.org/10.1016/j.jhazmat.2010.06.094.
Nishad, P.A., Bhaskarapillai, A., 2021. Antimony, a pollutant of emerging concern: a review on industrial sources and remediation technologies. Chemosphere 277, 130252. https://doi.org/10.1016/j.chemosphere.2021.130252.
Ociński, D., Mazur, P., 2020. Highly efficient arsenic sorbent based on residual from water deironing – sorption mechanisms and column studies. J. Hazard. Mater. 382, 121062. https://doi.org/10.1016/j.jhazmat.2019.121062.
Park, J.-H., et al., 2021. Adsorption behavior of arsenic onto lignin-based biochar decorated with zinc. Colloids Surf. A Physicochem. Eng. Asp. 626, 127095. https://doi.org/10.1016/j.colsurfa.2021.127095.
Patel, H., 2019. Fixed-bed column adsorption study: a comprehensive review. Appl Water Sci 9 (3), 1–17.
Patel, H., 2021. Review on solvent desorption study from exhausted adsorbent. J. Saudi Chem. Soc. 25 (8), 101302. https://doi.org/10.1016/j.jscs.2021.101302.
Patel, R., et al., 2019. Elimination of fluoride, arsenic, and nitrate from water through adsorption onto Nano-adsorbent: a review. Curr. Nanosci. 15. https://doi.org/10.2174/1573413715666190101113651.
Pathan, S., Bose, S., 2020. Biopolymer based hydrogels for arsenic removal. Curr. Sci. 118 (10), 1540–1546.
Pauling, L., 1933. The formulas of antimonic acid and the antimonates. J. Am. Chem. Soc. 55 (5), 1895–1900. https://doi.org/10.1021/ja01332a016.
Pehlivan, E., et al., 2013. Sugarcane bagasse treated with hydrous ferric oxide as a potential adsorbent for the removal of As(V) from aqueous solutions. Food Chem. 138 (1), 133–138. https://doi.org/10.1016/j.foodchem.2012.09.110.
Peng, Y., et al., 2021. Efficient removal of antimony(III) in aqueous phase by nano-Fe3O4 modified high-iron red mud: study on its performance and mechanism. Water 13 (6), 809.
Peng, L., et al., 2023. A critical review on adsorptive removal of antimony from waters: adsorbent species, interface behavior and interaction mechanism. Chemosphere 327, 138529. https://doi.org/10.1016/j.chemosphere.2023.138529.
Pintor, A.M.A., et al., 2018. Arsenate and arsenite adsorption onto iron-coated cork granulates. Sci. Total Environ. 642, 1075–1089. https://doi.org/10.1016/j.scitotenv.2018.06.170.
Pintor, A.M.A., et al., 2020. Removal of antimony from water by iron-coated cork granulates. Sep. Purif. Technol. 233, 116020. https://doi.org/10.1016/j.seppur.2019.116020.
Pintor, A.M.A., et al., 2021. Multicomponent adsorption of pentavalent As, Sb and P onto iron-coated cork granulates. J. Hazard. Mater. 406, 124339. https://doi.org/10.1016/j.jhazmat.2020.124339.
Pintor, A.M.A., et al., 2022. Establishing the state-of-the-art on the adsorption of coexisting pnictogens in water: a literature review. CHEMOSPHERE 286. https://doi.org/10.1016/j.chemosphere.2021.131947.
Pontius, F.W., 1994. Crafting a new arsenic rule. J. AWWA 86 (9), 6–104. https://doi.org/10.1002/j.1551-8833.1994.tb06243.x.
Pontoni, L., Fabbricino, M., 2012. Use of chitosan and chitosan-derivatives to remove arsenic from aqueous solutions-a mini review. Carbohydr. Res. 356, 86–92. https://doi.org/10.1016/j.carres.2012.03.042.
Qi, P., Pichler, T., 2017. Competitive adsorption of As(III), As(V), Sb(III) and Sb(V) onto ferrihydrite in multi-component systems: implications for mobility and distribution. J. Hazard. Mater. 330, 142–148. https://doi.org/10.1016/j.jhazmat.2017.02.016.
Qi, Z., et al., 2017. Synthesis of Ce(III)-doped Fe3O4 magnetic particles for efficient removal of antimony from aqueous solution. J. Hazard. Mater. 329, 193–204. https://doi.org/10.1016/j.jhazmat.2017.01.007.
Qiu, S., Yan, L., Jing, C., 2019. Simultaneous removal of arsenic and antimony from mining wastewater using granular TiO2: batch and field column studies. J. Environ. Sci. 75, 269–276. https://doi.org/10.1016/j.jes.2018.04.001.
Rathore, V.K., Mondal, P., 2017. Stabilization of arsenic and fluoride bearing spent adsorbent in clay bricks: preparation, characterization and leaching studies. J. Environ. Manage. 200, 160–169. https://doi.org/10.1016/j.jenvman.2017.05.081.
Raval, N.P., Kumar, M., 2022. Development of novel Core–shell impregnated polyuronate composite beads for an eco-efficient removal of arsenic. Bioresour. Technol. 364, 127918. https://doi.org/10.1016/j.biortech.2022.127918.
Runtti, H., et al., 2023. Removal of antimony from model solutions, mine effluent, and textile industry wastewater with Mg-rich mineral adsorbents. Environ. Sci. Pollut. Res. 30 (6), 14139–14154. https://doi.org/10.1007/s11356-022-23076-8.
Saldaña-Robles, A., et al., 2018. Effects of the presence of organic matter on the removal of arsenic from groundwater. J. Clean. Prod. 183, 720–728. https://doi.org/10.1016/j.jclepro.2018.02.161.
Saleh, T.A., Sarı, A., Tuzen, M., 2017. Effective adsorption of antimony(III) from aqueous solutions by polyamide-graphene composite as a novel adsorbent. Chem. Eng. J. 307, 230–238. https://doi.org/10.1016/j.cej.2016.08.070.
Sarı, A., Çıtak, D., Tuzen, M., 2010. Equilibrium, thermodynamic and kinetic studies on adsorption of Sb(III) from aqueous solution using low-cost natural diatomite. Chem. Eng. J. 162 (2), 521–527. https://doi.org/10.1016/j.cej.2010.05.054.
Sari, A., Tuzen, M., Kocal, İ., 2017. Application of chitosan-modified pumice for antimony adsorption from aqueous solution. Environ. Prog. Sustain. Energy 36 (6), 1587–1596. https://doi.org/10.1002/ep.12611.
Sarmah, S., et al., 2019. Adsorption of As(V) from water over a hydroxyl-alumina modified Paddy husk ash surface and its sludge immobilization. Water Air Soil Pollut. 230 (2), 32. https://doi.org/10.1007/s11270-019-4088-y.
Schweitzer, G.K., Pesterfield, L.L., 2010. The Aqueous Chemistry of the Elements. OUP USA.
Senthil Kumar, P., Ngueagni, P. Tsopbou, 2022. Chapter 15 - removal of volatile organic carbon and heavy metols through microbial approach. In: Shah, M., Rodriguez-Couto, S., Biswas, J. (Eds.), An Innovative Role of Biofiltration in Wastewater Treatment Plants (WWTPs). Elsevier, pp. 285–308. https://doi.org/10.1016/B978-0-12-823946-9.00016-4.
Setyono, D., Valiyaveettil, S., 2014. Chemically modified sawdust as renewable adsorbent for arsenic removal from water. ACS Sustain. Chem. Eng. 2 (12), 2722–2729. https://doi.org/10.1021/sc500458x.

Shaji, E., et al., 2021. Arsenic contamination of groundwater: a global synopsis with focus on the Indian peninsula. Geosci. Front. 12 (3), 101079. https://doi.org/10.1016/j.gsf.2020.08.015.
Shakoor, M.B., et al., 2018. Arsenic removal by natural and chemically modified water melon rind in aqueous solutions and groundwater. Sci. Total Environ. 645, 1444–1455. https://doi.org/10.1016/j.scitotenv.2018.07.218.
Siddiqui, S.I., Naushad, M., Chaudhry, S.A., 2019. Promising prospects of nanomaterials for arsenic water remediation: a comprehensive review. Process Saf. Environ. Prot. 126, 60–97. https://doi.org/10.1016/j.psep.2019.03.037.
Simeonidis, K., et al., 2017. Efficiency of Iron-based oxy-hydroxides in removing antimony from groundwater to levels below the drinking water regulation limits. Sustainability 9 (2), 238.
Simsek, E.B., et al., 2018. Novel composite sorbents based on carbon fibers decorated with ferric hydroxides – simultaneous removal of antimonate and arsenate from aqueous solutions. Water Supply 19 (3), 838–845. https://doi.org/10.2166/ws.2018.130.
Smichowski, P., Madrid, Y., Cámara, C., 1998. Analytical methods for antimony speciation in waters at trace and ultratrace levels. A review. Fresenius J. Anal. Chem. 360 (6), 623–629. https://doi.org/10.1007/s002160050770.
Smith, A.H., Smith, M.M.H., 2004. Arsenic drinking water regulations in developing countries with extensive exposure. Toxicology 198 (1), 39–44. https://doi.org/10.1016/j.tox.2004.02.024.
Sorg, T.J., et al., 2017. Regenerating an arsenic removal Iron-bed adsorptive media system, part 2: performance and cost. J. Am. Water Works Assoc. 109 (5), E122–e128. https://doi.org/10.5942/jawwa.2017.109.0046.
Srivastav, A.L., et al., Biochar adsorbents for arsenic removal from water environment: a review. Bull. Environ. Contam. Toxicol.DOI:https://doi.org/10.1007/s00128-021-03374-6.
Sun, F., et al., 2014. Biosorption of antimony(V) by freshwater cyanobacteria Microcystis from Lake Taihu, China: effects of pH and competitive ions. Environ. Sci. Pollut. Res. 21 (9), 5836–5848. https://doi.org/10.1007/s11356-014-2522-7.
SW, E., 1992. 846. Test method 1311: toxicity characteristic leaching procedure, part of test methods for evaluating solid waste, physical/chemical methods. Environ. Protect. Agency 1311-01–1311-35.
Tamaddoni Moghaddam, S., et al., 2023. Effect of reaction parameters on arsenic removal capacity from aqueous solutions using modified magnetic PU foam nanocomposite. Results Mater. 17, 100373. https://doi.org/10.1016/j.rinma.2023.100373.
Thakur, N., Armstrong, D.W., 2021. Arsenic sequestration by iron oxide coated geopolymer microspheres. J. Clean. Prod. 291, 125931. https://doi.org/10.1016/j.jclepro.2021.125931.
Thomas, H.C., 1944. Heterogeneous ion exchange in a flowing system. J. Am. Chem. Soc. 66 (10), 1664–1666. https://doi.org/10.1021/ja01238a017.
Tian, Y., et al., 2011. Synthesis of magnetic wheat straw for arsenic adsorption. J. Hazard. Mater. 193, 10–16. https://doi.org/10.1016/j.jhazmat.2011.04.093.
Tresintsi, S., et al., 2014. A novel approach for arsenic adsorbents regeneration using MgO. J. Hazard. Mater. 265, 217–225. https://doi.org/10.1016/j.jhazmat.2013.12.003.
Tuutijärvi, T., et al., 2012. Maghemite nanoparticles for as(V) removal: desorption characteristics and adsorbent recovery. Environ. Technol. 33 (16), 1927–1936. https://doi.org/10.1080/09593330.2011.651162.
Tuzen, M., et al., 2009. Characterization of biosorption process of As(III) on green algae Ulothrix cylindricum. J. Hazard. Mater. 165 (1), 566–572. https://doi.org/10.1016/j.jhazmat.2008.10.020.
Uluozlu, O.D., Sarı, A., Tuzen, M., 2010. Biosorption of antimony from aqueous solution by lichen (Physcia tribacia) biomass. Chem. Eng. J. 163 (3), 382–388. https://doi.org/10.1016/j.cej.2010.08.022.
Ungureanu, G., et al., 2015. Arsenic and antimony in water and wastewater: overview of removal techniques with special reference to latest advances in adsorption. J. Environ. Manage. 151, 326–342. https://doi.org/10.1016/j.jenvman.2014.12.051.
Ungureanu, G., et al., 2016. Antimony oxyanions uptake by green marine macroalgae. J. Environ. Chem. Eng. 4 (3), 3441–3450. https://doi.org/10.1016/j.jece.2016.07.023.
USPHS, 1943. Public health service drinking water standards. Public Health Rep. (1896-1970) 58 (3), 69–82.
Vakili, M., et al., 2019. Regeneration of chitosan-based adsorbents used in heavy metal adsorption: a review. Sep. Purif. Technol. 224, 373–387. https://doi.org/10.1016/j.seppur.2019.05.040.
van Genuchten, C.M., et al., 2022. LCA of disposal practices for arsenic-bearing Iron oxides reveals the need for advanced arsenic recovery. Environ. Sci. Technol. 56 (19), 14109–14119. https://doi.org/10.1021/acs.est.2c05417.
Verbinnen, B., et al., 2015. Recycling of spent adsorbents for oxyanions and heavy metal ions in the production of ceramics. Waste Manag. 45, 407–411. https://doi.org/10.1016/j.wasman.2015.07.006.
Vieira, B.R.C., et al., 2017. Arsenic removal from water using iron-coated seaweeds. J. Environ. Manage. 192, 224–233. https://doi.org/10.1016/j.jenvman.2017.01.054.
Vijayaraghavan, K., Balasubramanian, R., 2011. Antimonite removal using marine algal species. Ind. Eng. Chem. Res. 50 (17), 9864–9869. https://doi.org/10.1021/ie200776m.
Wang, S., Gao, B., Li, Y., 2016. Enhanced arsenic removal by biochar modified with nickel (Ni) and manganese (Mn) oxyhydroxides. J. Ind. Eng. Chem. 37, 361–365. https://doi.org/10.1016/j.jiec.2016.03.048.
Wang, L., et al., 2018. Enhanced antimonate (Sb(V)) removal from aqueous solution by La-doped magnetic biochars. Chem. Eng. J. 354, 623–632. https://doi.org/10.1016/j.cej.2018.08.074.
Wang, J., et al., 2022. Reductive removal of As(V) and As(III) from aqueous solution by the UV/sulfite process: recovery of elemental arsenic. Water Res. 223, 118981. https://doi.org/10.1016/j.watres.2022.118981.
Wang, Z., et al., 2023a. Efficient removal of arsenate from water using electrospun polyethylenimine/polyvinyl chloride nanofiber sheets. React. Funct. Polym. 184, 105514. https://doi.org/10.1016/j.reactfunctpolym.2023.105514.
Wang, K., et al., 2023b. Molecular-scale characterization of groundwater treatment sludge from around the world: implications for potential arsenic recovery. Water Res. 245, 120561. https://doi.org/10.1016/j.watres.2023.120561.
WHO, 2017. Guidelines for Drinking-water Quality: Fourth Edition Incorporating First Addendum, 4th + 1st add ed. World Health Organization, Geneva.
WHO, 2022. Guidelines for Drinking-Water Quality: Incorporating the First and Second Addenda. World Health Organization, Geneva.
Wilson, S.C., et al., 2010. The chemistry and behaviour of antimony in the soil environment with comparisons to arsenic: a critical review. Environ. Pollut. 158 (5), 1169–1181. https://doi.org/10.1016/j.envpol.2009.10.045.
World Health, O, 1958. International Standards for Drinking-Water. World Health Organization, Geneva.
World Health, O, 1993. Guidelines for Drinking-Water Quality: Volume 1: Recommendations, 2nd ed. World Health Organization, Geneva.
Xi, J., He, M., Lin, C., 2010. Adsorption of antimony(V) on kaolinite as a function of pH, ionic strength and humic acid. Environ. Earth Sci. 60 (4), 715–722. https://doi.org/10.1007/s12665-009-0209-z.
Xu, Z., Cai, J.-g., Pan, B.-c., 2013. Mathematically modeling fixed-bed adsorption in aqueous systems. J. Zheijang Univ. Sci. A 14 (3), 155–176. https://doi.org/10.1631/jzus.A1300029.
Xu, R., et al., 2022. Simultaneous removal of antimony(III/V) and arsenic(III/V) from aqueous solution by bacteria–mediated kaolin@Fe–Mn binary (hydr)oxides composites. Appl. Clay Sci. 217, 106392. https://doi.org/10.1016/j.clay.2021.106392.
Yadav, M.K., et al., 2022. A review on the management of arsenic-laden spent adsorbent: insights of global practices, process criticality, and sustainable solutions. Environ. Technol. Innov. 27, 102500. https://doi.org/10.1016/j.eti.2022.102500.
Yan, G., Viraraghavan, T., Chen, M., 2001. A new model for heavy metal removal in a biosorption column. Adsorpt. Sci. Technol. 19 (1), 25–43.
Yan, X.-L., et al., 2008. Arsenic transformation and volatilization during incineration of the hyperaccumulator Pteris vittata L. Environ. Sci. Technol. 42 (5), 1479–1484. https://doi.org/10.1021/es0717459.
Yan, L., Hu, S., Jing, C.Y., 2016. Recent progress of arsenic adsorption on TiO2 in the presence of coexisting ions: a review. J. Environ. Sci. 49, 74–85. https://doi.org/10.1016/j.jes.2016.07.007.
Yan, R., et al., 2020. Effective adsorption of antimony from aqueous solution by cerium hydroxide loaded on Y-tape molecular sieve adsorbent: performance and mechanism. Colloids Surf. A Physicochem. Eng. Asp. 604, 125317. https://doi.org/10.1016/j.colsurfa.2020.125317.
Yang, X., et al., 2015a. Adsorption of trivalent antimony from aqueous solution using graphene oxide: kinetic and thermodynamic studies. J. Chem. Eng. Data 60 (3), 806–813. https://doi.org/10.1021/je5009262.
Yang, X., Shi, Z., Liu, L., 2015b. Adsorption of Sb(III) from aqueous solution by QFGO particles in batch and fixed-bed systems. Chem. Eng. J. 260, 444–453. https://doi.org/10.1016/j.cej.2014.09.036.
Yang, X., Xia, L., Song, S., 2016. Arsenic adsorption from water using graphene-based materials as adsorbents: a critical review. Surf. Rev. Lett. 24 (01), 1730001. https://doi.org/10.1142/S0218625X17300015.
Yang, K.L., et al., 2017. Preparation and application of iron. based composite materials for the removal of antimony from aqueous solution. Prog. Chem. 29 (11), 1407–1421. https://doi.org/10.7536/PC170634.
Yang, K., et al., 2018. Removal of Sb(V) from aqueous solutions using Fe-Mn binary oxides: the influence of iron oxides forms and the role of manganese oxides. Chem. Eng. J. 354, 577–588. https://doi.org/10.1016/j.cej.2018.08.069.
Yang, B., et al., 2021a. Preparation of a spindle δ-MnO2@Fe/Co-MOF-74 for effective adsorption of arsenic from water. Colloids Surf. A Physicochem. Eng. Asp. 629, 127378. https://doi.org/10.1016/j.colsurfa.2021.127378.
Yang, K., et al., 2021b. Efficient removal of Sb(V) in textile wastewater through novel amorphous Si-doped Fe oxide composites: phase composition, stability and adsorption mechanism. Chem. Eng. J. 407, 127217. https://doi.org/10.1016/j.cej.2020.127217.
Yang, Y., et al., 2024. Deep separation of arsenic and alkali from alkaline arsenic containing solution using hydrothermal lime precipitation method. J. Environ. Chem. Eng. 12 (2), 112294. https://doi.org/10.1016/j.jece.2024.112294.
Yeo, K.F.H., et al., 2021. Arsenic removal from contaminated water using natural adsorbents: a review. COATINGS 11 (11). https://doi.org/10.3390/coatings11111407.
Yeo, K.F.H., et al., 2022a. Fast arsenate As(V) adsorption and removal from water using aluminium Al(III) fixed on Kapok fibres. Environmental Pollution 314, 120236. https://doi.org/10.1016/j.envpol.2022.120236.
Yeo, K.F.H., et al., 2022b. Adsorption performance of Fe(III) modified kapok fiber for As (V) removal from water. Sep. Purif. Technol. 287, 120494. https://doi.org/10.1016/j.seppur.2022.120494.
Yoon, Y.H., Nelson, J.H., 1984. Application of gas adsorption kinetics. I. A theoretical model for respirator cartridge service life. Am. Ind. Hyg. Assoc. J. 45 (8), 509–516. https://doi.org/10.1080/15298668491400197.

Yu, Y., et al., 2018. Rare-earth metal based adsorbents for effective removal of arsenic from water: a critical review. Crit. Rev. Environ. Sci. Technol. 48 (22–24), 1127–1164. https://doi.org/10.1080/10643389.2018.1514930.

Zaimee, M.Z., Sarjadi, M.S., Rahman, M.L., 2021. Heavy metals removal from water by efficient adsorbents. Water 13 (19). https://doi.org/10.3390/w13192659.

Zeng, H., et al., 2024. Facile preparation of maghemite based on iron sludge for arsenic removal from water. Sci. Total Environ. 906, 167575. https://doi.org/10.1016/j.scitotenv.2023.167575.

Zhang, F., et al., 2016. Efficient arsenate removal by magnetite-modified water hyacinth biochar. Environ. Pollut. 216, 575–583. https://doi.org/10.1016/j.envpol.2016.06.013.

Zhang, X., et al., 2021. Insights into adsorptive removal of antimony contaminants: functional materials, evaluation and prospective. J. Hazard. Mater. 418, 126345. https://doi.org/10.1016/j.jhazmat.2021.126345.

Zhang, L., et al., 2022. The effect of co-pyrolysis temperature for iron-biochar composites on their adsorption behavior of antimonite and antimonate in aqueous solution. Bioresour. Technol. 347, 126362. https://doi.org/10.1016/j.biortech.2021.126362.

Zhang, K., et al., 2023a. Highly efficient and robust monolith of a metal–organic framework hybrid aerogel for the removal of antimony from water. ACS ES&T Eng. 3 (1), 45–56. https://doi.org/10.1021/acsestengg.2c00240.

Zhang, C., et al., 2023b. Efficient removal of antimonate and antimonite by a novel lanthanum-manganese binary oxide: performance and mechanism. J. Hazard. Mater. 442, 130132. https://doi.org/10.1016/j.jhazmat.2022.130132.

Zhao, Y., et al., 2023. Removal of As(V) from aqueous solution using modified Fe₃O₄ nanoparticles. R. Soc. Open Sci. 10 (1), 220988. https://doi.org/10.1098/rsos.220988.

Zhu, H., et al., 2021. Removal of antimony(V) from drinking water using nZVI/AC: optimization of batch and fix bed conditions. Toxics 9 (10), 266.

Zhu, T., et al., 2022. Synthesis of novel hydrated ferric oxide biochar nanohybrids for efficient arsenic removal from wastewater. Rare Metals 41 (5), 1677–1687. https://doi.org/10.1007/s12598-021-01920-z.